



Competitive intransitivity, population interaction structure, and strategy coexistence



Robert A. Laird ^{a,*}, Brandon S. Schamp ^b

^a Department of Biological Sciences, University of Lethbridge, Lethbridge, AB, Canada T1K 3M4

^b Department of Biology, Algoma University, Sault Ste. Marie, ON, Canada P6A 2G3

HIGHLIGHTS

- Intransitive competition (as in the game rock–paper–scissors) promotes coexistence.
- Spatial structure can enhance intransitivity-mediated coexistence.
- We model intransitivity on spatial, small-world, and regular random graphs.
- Coexistence that occurs in spatial lattices is inhibited as network disorder grows.
- Threshold disorder for monoculture is positively related to population size.

ARTICLE INFO

Article history:

Received 27 August 2014

Received in revised form

30 September 2014

Accepted 7 October 2014

Available online 18 October 2014

Keywords:

Cyclical population dynamics

Evolutionary graph theory

Quenched randomness

Rock–paper–scissors

Small-world networks

ABSTRACT

Intransitive competition occurs when competing strategies cannot be listed in a hierarchy, but rather form loops—as in the game rock–paper–scissors. Due to its cyclic competitive replacement, competitive intransitivity promotes strategy coexistence, both in rock–paper–scissors and in higher-richness communities. Previous work has shown that this intransitivity-mediated coexistence is strongly influenced by spatially explicit interactions, compared to when populations are well mixed. Here, we extend and broaden this line of research and examine the impact on coexistence of intransitive competition taking place on a continuum of small-world networks linking spatial lattices and regular random graphs. We use simulations to show that the positive effect of competitive intransitivity on strategy coexistence holds when competition occurs on networks toward the spatial end of the continuum. However, in networks that are sufficiently disordered, increasingly violent fluctuations in strategy frequencies can lead to extinctions and the prevalence of monocultures. We further show that the degree of disorder that leads to the transition between these two regimes is positively dependent on population size; indeed for very large populations, intransitivity-mediated strategy coexistence may even be possible in regular graphs with completely random connections. Our results emphasize the importance of interaction structure in determining strategy dynamics and diversity.

© 2014 Elsevier Ltd. All rights reserved.

1. Introduction

A main question in community ecology is how species can coexist despite differences in competitive ability (Chesson, 2000; Huston, 1994; Hutchinson, 1959; Tokeshi, 1999; Wilson, 1990, 2011). Many mechanisms have been proposed, most of which invoke exogenous factors that lessen the impact of competition. Here, we deal with a mechanism that is endogenous to the competitive system itself: competitive intransitivity (Gilpin, 1975;

May and Leonard, 1975). Using simulation models, we consider intransitive competition and coexistence among ‘strategies’, a general term referring to any entities (most commonly species, but also including physiological, behavioral, life-historical, and even ideological variants or strains) that compete, and in doing so, have the potential to exclude one another from their environment.

Transitive competition occurs when strategies can be listed in a strict hierarchy in which strategies higher on the list outcompete those lower on the list, but not vice versa. Transitive competition appeals to the intuition: If strategy *A* outcompetes strategy *B*, and *B* outcompetes *C*, it makes intuitive sense that *A* outcompetes *C*. However, this is not necessarily the case. The simplest counter-example, and, thus, the simplest example of intransitive competition,

* Corresponding author.

E-mail address: robert.laird@uleth.ca (R.A. Laird).

is the game of rock–paper–scissors, in which Paper beats Rock, Rock beats Scissors, and Scissors beats Paper. In populations composed of these three strategies, cyclic dynamics occur, leading to the potential for the coexistence of all three, provided the fluxes in the cycles are not too strong (e.g., Gilpin, 1975; May and Leonard, 1975; Vandermeer, 2011). Rock–paper–scissors and its descendants are fundamentally frequency-dependent phenomena, and the study of intransitive competition and its effects on coexistence are important facets of evolutionary game theory (Hofbauer and Sigmund, 1998; Maynard Smith, 1982; Nowak, 2006; Sigmund, 2010). Extending beyond theoretical considerations, real-world empirical examples of intransitivity-mediated coexistence now span many branches of the tree of life, including within or among bacteria (Kerr et al., 2002; Kirkup and Riley, 2004; Nahum et al., 2011), vertebrate (Bleay et al., 2007; Sinervo and Lively, 1996; Sinervo et al., 2007) and invertebrate animals (Buss, 1976, 1980; Buss and Jackson, 1979; Dunstan and Johnson, 2005; Jackson and Buss, 1975; Rubin, 1982), coralline algae (Buss, 1976, 1980; Buss and Jackson, 1979), plants (Lankau and Strauss, 2007; Taylor and Aarssen, 1990), and possibly phytoplankton (Huisman and Weissing, 2001b) and yeasts (Paquin and Adams, 1983). Intransitivity also bears upon important issues in human decision-making procedures (Kendall and Babington Smith, 1940; May, 1954; Tversky, 2004), including voting systems (Arrow, 1950; Hughes, 1980; Riker, 1961).

Although classic theory and simulation papers typically deal with three-strategy intransitivity (e.g., Czárán et al., 2002; Durrett and Levin, 1998; Freat and Abraham, 2001; May and Leonard, 1975; Neumann and Schuster, 2007; Schreiber and Killingback, 2013; Szabó et al., 2004; Tainaka, 1988), and many of the empirical examples above involve variants of rock–paper–scissors (e.g., toxic, resistant, and susceptible strains of *Escherichia coli* (Kerr et al., 2002); orange, yellow, and blue chromo-behavioral morphs of side-blotched lizards (Sinervo and Lively, 1996)), the study of the relationship between competitive intransitivity and coexistence can be generalized to more strategy-rich communities (Gilpin, 1975; Huisman and Weissing, 1999, 2001a,b; Huisman et al., 2001; Karlson and Jackson, 1981; Laird and Schamp, 2006, 2008, 2009). This reflects the facts that (a) in many systems, multi-strategy communities are common (e.g., multi-species communities in biological systems or multiple ideologies in the socio-political sphere), and (b) intransitivity readily results from typical traits of these multi-strategy communities, such as trade-offs during exploitation competition (Huisman and Weissing, 1999, 2001a,b; Huisman et al., 2001) and allelopathy (Kerr et al., 2002; Lankau and Strauss, 2007). When this generalization is made, the transitive-intransitive dichotomy gives way to a series of intermediately intransitive competition scenarios that becomes increasingly continuous as the number of strategies grows. The level of intransitivity across this continuum can be quantified using an index (Bezembinder, 1981; Kendall and Babington Smith, 1940; Laird and Schamp, 2006, 2008; Petraitis, 1979; Slater, 1961), making it straightforward to examine quantitatively the relationship between strategy coexistence and intransitivity. As would be expected by extrapolating the lesson of three-strategy coexistence, competitive intransitivity also promotes strategy coexistence when more than three strategies are involved (e.g., Allesina and Levine, 2011; Karlson and Jackson, 1981; Laird and Schamp, 2006, 2008, 2009; Rojas-Echenique and Allesina, 2011; but see Vandermeer and Yitbarek, 2012 for a counterexample). Thus, intransitivity may play an important role in maintaining diversity in communities of varying types.

The simplest intransitivity models within evolutionary game theory have no interaction structure; rather, they behave according to mean-field assumptions, whereby strategies embedded in large, well-mixed communities interact according to their relative abundances and the principle of mass action (e.g., Allesina and

Levine, 2011; Freat and Abraham, 2001; Gilpin, 1975; May and Leonard, 1975). Allesina and Levine (2011) provide an effective means to deal with these models and predict the outcome of competition. However, paralleling the rising interest in the effect of interaction structure in evolutionary game theory in general (particularly in models designed to understand the evolution of cooperation, and, specifically, how cooperators and defectors can coexist: Hauert, 2001, 2002, 2006; Hauert and Doebeli, 2004; Laird, 2011, 2012, 2013; Laird et al., 2013; Lieberman et al., 2005; Nowak and May, 1992, 1993; Nowak et al., 1994a,b; Szabó and Töke, 1998; Szolnoki et al., 2008), there is a proliferation of studies of intransitive competition in which mean-field assumptions are relaxed (e.g., Durrett and Levin, 1998; Freat and Abraham, 2001; Károlyi et al., 2005; Laird, 2014; Reichenbach et al., 2007; Schreiber and Killingback, 2013; Szabó et al., 2004; Szolnoki and Szabó, 2004; Tainaka, 2001; Zhang et al., 2009). The general lesson is that variation in interaction structure can modify greatly the outcome of competition in intransitive systems.

Spatial structure, whereby individuals interact preferentially (or solely) with their nearest neighbors, is one of the main types of interaction structure that has been modeled in the context of intransitivity-mediated strategy coexistence (Durrett and Levin, 1998; Freat and Abraham, 2001; Kerr et al., 2002; Laird and Schamp, 2006, 2008, 2009). This type of structure is particularly relevant in biological systems whose members are largely sessile and confined to a two-dimensional substrate (e.g., biofilms (Kerr et al., 2002); encrusting benthic invertebrates (Dunstan and Johnson, 2005; Wootton, 2001)). Generally speaking, simulations predict that spatially explicit interactions enhance intransitivity-mediated coexistence (e.g., Durrett and Levin, 1998; Freat and Abraham, 2001; Kerr et al., 2002; but see Laird and Schamp, 2008; Rojas-Echenique and Allesina, 2011). This prediction is supported by key experimental data (e.g., Kerr et al., 2002).

The advent of evolutionary graph theory (Lieberman et al., 2005; Nowak, 2006; Perc et al., 2013; Szabó and Fáth, 2007) provides a framework whereby individuals interacting in arbitrarily structured populations can be studied. In this manner, spatial structure becomes a special case of interaction topology. As with spatial extensions of evolutionary game theory, more general graph-theoretical extensions are strongly influenced, in terms of approach, by recent models of the evolution of cooperation (Du et al., 2009; Hadzibeganovic et al., 2012; Lieberman et al., 2005; Lima et al., 2009; Nowak, 2006; Pacheco et al., 2006; Szolnoki and Perc, 2009; Szolnoki et al., 2008; Wang et al., 2006). In evolutionary graph theory, individuals interact with a subset of the population/community to which they belong, though not necessarily with those that are spatially close. In terms of intransitivity-mediated strategy coexistence, evolutionary graph theory is most relevant in humans and other species in which the existence of social networks can lead to complex population-level interaction structures. Additionally, there are other systems (biological, social, and technological) where interactions on graphs or networks are the norm (Watts and Strogatz, 1998). Finally, even in systems where aspatial interaction graphs are unlikely, modeling the outcome of interactions on such graphs may provide a point of contrast—a tool with which salient aspects of more realistic interaction structures can be examined in detail (e.g., Laird, 2014).

Szabó et al. (2004) and Szolnoki and Szabó (2004) consider the rock–paper–scissors game along a continuum of regular, small-world networks (Watts and Strogatz, 1998) ranging from spatial lattices to regular random graphs (also see Kuperman and Abramson, 2001; Laird, 2014; Ying et al., 2007). They show that by increasing quenched randomness (profitably thought of as an inverse measure of inherent spatial structure), disparate parts of the network become synchronized, leading to a Hopf bifurcation at which the strategy frequency dynamics transition from a

stationary state to a limit cycle. Further increases in quenched randomness lead to an increasing (but decelerating) amplitude of oscillations in this limit cycle, resulting in the potential for strategy extinctions, and inevitable monoculture, unless the population is sufficiently large. (Szabó et al. (2004) also show a rather similar pattern with increased annealed randomness, which connects spatial lattices with well-mixed, mean-field dynamics. In an interesting convergence from a meta-community as opposed to graph-theoretical model, Schreiber and Killingback (2013) discovered a critical dispersal rate beyond which strategy coexistence was no longer possible.)

Here, we extend the work of our predecessors (Kuperman and Abramson, 2001; Szabó et al., 2004; Szolnoki and Szabó, 2004; Ying et al., 2007) to communities with as many as 101 strategies, reflecting the fact that many systems, especially biological communities, often exhibit extraordinary degrees of coexistence. Our motivation is to determine how the degree of intransitivity and population structure interact to determine strategy coexistence in finite competitive communities. We show that when quenched randomness is below a critical value, as in spatially structured systems, long-term strategy richness is positively related to intransitivity, as predicted by previous research (Laird and Schamp, 2006, 2008). Above the critical value, however, the increasing violence of strategy oscillations leads to random extinctions and the prevalence of monocultures. Further, building on the notion that the amplitude in strategy oscillations rises more slowly with quenched randomness in large compared to small populations (Szabó et al., 2004), we show that the critical value increases with population size and may even disappear altogether in very large populations. Our results emphasize the importance of interaction structure and population size in determining strategy dynamics and diversity.

2. Methods

2.1. Graph structure

In our model, competition is characterized by two graphs, the interaction graph and the tournament graph. Examining the outcome of competition when these two types of graphs are varied is one of the main goals of this paper.

2.2. Interaction graph and quenched randomness (Q)

The interaction graph describes the population interaction structure; i.e., it determines who interacts with whom. Individuals are placed at nodes, and edges connect individuals that interact. It is possible to have complete interaction graphs, where every node is connected to every other node; in large populations, interactions on such graphs approximate mean-field dynamics. However, here we consider incomplete (albeit connected) graphs in which each node is connected only to a subset of the other nodes. Specifically, we consider k -regular connected graphs, where k is the number of other nodes to which every node is connected (i.e., the degree or neighborhood size). Incomplete graphs are appropriate in many real situations: both biological and human systems are rarely so well mixed that all pairs of individuals are equally likely to interact; rather, individuals are more likely to interact with those who are spatially close, with those to whom they are socially connected, or both, to varying degrees.

We investigate a continuum of interaction graphs along a gradient of quenched randomness (Szabó et al., 2004; Szolnoki and Szabó, 2004), ranging from graphs representing spatial lattices to regular random graphs. Quenched randomness is applied by breaking a proportion Q of the edges in a two-dimensional lattice

and then randomly joining pairs of the resulting half-edges so that every node continues to have exactly k edges emanating from it. When $Q=0$, the original lattice is preserved. When $Q=1$, the resulting interaction graph is a regular random graph. When $0 < Q < 1$, the resulting interaction graph is a small-world network (e.g., Fig. A1) (Szabó and Fáth, 2007; Szabó et al., 2004; Szolnoki and Szabó, 2004; Watts and Strogatz, 1998). Thus, as Q increases from 0, the resulting graphs become progressively detached from the inherent spatial properties of the original lattices used to create them; they also have lower characteristic path lengths ('degrees of separation') and clustering coefficients ('cliquishness')—traits Watts and Strogatz (1998) argue are common over a diverse suite of large networks in nature. Following intransitive competition on this continuum of graphs allows us to predict the characteristics of the sorts of systems where intransitivity-mediated coexistence is more likely to occur.

We consider interaction graphs with $k=3, 4, 6$, or 8 , as the number of neighbors is known to be important in the rock–paper–scissors game (Szolnoki and Szabó, 2004). Interactions on $k=3, 4$, or 6 lattices are equivalent to interactions taking place between bordering cells arrayed as tessellated equilateral triangles, squares, or regular hexagons (i.e., the three types of regular tessellations on the plane) in cellular automaton models. Interactions on $k=8$ lattices are equivalent to interactions taking place between bordering cells, and between cells sharing a common corner, in cellular automaton models composed of tessellated squares. The neighborhoods that arise in the $k=4$ and $k=8$ cases have special names in the context of cellular automata: the von Neumann neighborhood and the Moore neighborhood, respectively (Durrett and Levin, 1994).

2.3. Tournament graph and relative intransitivity (RI)

The tournament graph describes how individuals bearing different strategies fare against one another when they interact. It is a complete, oriented graph in which edges connecting pairs of nodes (strategies) point from competitive subordinates to competitive dominants. This allows us to generalize the rock–paper–scissors game into more strategy-rich scenarios (e.g., rock–paper–scissors–lizard–Spock¹ (Vukov et al., 2013) and beyond). While the most celebrated examples of intransitivity-mediated coexistence involve three strategies (e.g., Kerr et al., 2002; Sinervo and Lively, 1996), many of the systems in which it is hypothesized to be important (corals, phytoplankton) are considerably more rich.

The topology of the tournament graph determines the level of competitive intransitivity (Laird and Schamp, 2009). We measure intransitivity using the relative intransitivity index (RI) (Laird and Schamp, 2008). To do so, the tournament graph is first converted to a tournament matrix $M=[m_{ij}]$, in which $m_{ij}=1$ if strategy i is dominant to strategy j , and $m_{ij}=0$ otherwise (i.e., highly asymmetrical or unbalanced competition; for an approach that considers a gradient in competitive balance, see Vandermeer and Yitbarek, 2012). For each strategy i , $w_i=\sum_j m_{ij}$ determines the total number of wins that strategy has against all the other strategies. The sequence of all w_i is the 'score sequence' of M . Score sequences are presented in non-descending order. Competitive hierarchies include both highly dominant and highly subordinate strategies and therefore have score sequences with relatively high sums of squared deviations (or, equivalently, variance; Laird and Schamp, 2006, 2008). For example, a hierarchy of seven strategies has the score sequence $\{0, 1, 2, 3, 4, 5, 6\}$ and a sum of squared deviations (hereafter SS) of $\sum_i (w_i - w_{avg})^2 = 28$. Highly intransitive

¹ Often attributed to S. Kass and K. Bryla (<http://www.samkass.com/theories/RPSSL.html>).

tournaments, on the other hand, are composed of more-or-less evenly matched strategies, leading to score sequences with relatively low sums of squared deviations; a perfectly intransitive seven-strategy tournament has the score sequence {3, 3, 3, 3, 3, 3, 3}, resulting in $SS=0$ (e.g., Fig. A2). Relative intransitivity is calculated as $RI=1-(SS_{\text{obs}}-SS_{\text{min}})/(SS_{\text{max}}-SS_{\text{min}})$, where SS_{obs} is the SS of the observed score sequence, and SS_{max} and SS_{min} are, respectively, the greatest- and least-possible SS values of score sequences derived from tournaments composed of the same number of strategies as the observed tournament. Thus, RI is a rational number between 0 and 1 with large values corresponding to more intransitive tournaments. Following Kendall and Babington Smith (1940), $SS_{\text{min}}=0$ when the number of strategies, s , is odd and $s/4$ when s is even. Similarly, $SS_{\text{max}}=(s^3-s)/12$ (also see Appendix A of Rojas-Echenique and Allesina, 2011).

Interestingly, RI is exactly equivalent to $1-\zeta$, where ζ is Kendall and Babington Smith's (1940) coefficient of consistence, a metric originally designed to test for the consistency of experimental subjects when presented with a series of paired comparisons. Kendall and Babington Smith (1940) demonstrate that during competitive reversals, where the entries of m_{ij} and m_{ji} are swapped ($i \neq j$), the smallest possible non-zero change to SS_{obs} is 2. This implies that the smallest possible increment of RI is $\phi=24/(s^3-s)$ when s is odd and $\phi=24/(s^3-4s)$ when s is even. Kendall and Babington Smith (1940) make the further claim that all the increments are possible, constrained only by SS_{max} and SS_{min} , implying that for any given $s \geq 3$, there exist tournaments whose RI 's encompass all the values $d\phi$, where d is an integer between 0 and ϕ^{-1} , inclusive. This claim is consistent with our preliminary investigations that show that for $s \in \{3, 4, \dots, 101\}$, it is possible to generate tournaments with all candidate $RI=d\phi$ values (not shown). Furthermore, d is equal to the number of intransitive triads in sub-graphs of M , and ϕ^{-1} the maximum number of such triads (Kendall and Babington Smith, 1940), demonstrating that RI has an intuitive link with M 's intransitivity, and not merely a convenient statistical one (Fig. A2).

Finally, we note that it is also possible to study graphs that feature non-tournament strategy-competition outcomes (e.g., those with ties or with probabilistic outcomes; Vandermeer and Yitbarek, 2012); however, these "introduce complications of a most intractable kind" (Kendall and Babington Smith, 1940, p. 325), and we do not consider them at this juncture.

2.4. Simulations

We consider square lattices with periodic boundaries (and the small-world and regular random graphs that emerge from them when $Q > 0$) with $N=250^2=62,500$ nodes and $31,250k$ edges (i.e., $Nk/2$ edges). At the start of each model run, all the nodes of a new, randomly generated interaction graph of quenched randomness Q are populated randomly and independently with s strategies which interact according to a new, randomly generated tournament graph of relative intransitivity RI . We investigate initial strategy richness values of $s=6, 7, 20, 21, 100$, and 101 (i.e., even-odd pairs of low, medium, and high initial strategy richness). The most initially strategy-rich scenario ($s=101$) is detailed in the main text²; all are considered in Fig. A3. Our motivation for using even-odd pairs is that only odd tournament sizes can have totally uniform score sequences (i.e., $SS_{\text{obs}}=0$), leading to greater potential for intransitivity-mediated coexistence.

In every time-step, individuals located at two nodes sharing an edge, X and Y , are chosen at random. If, according to the

tournament graph, X 's strategy defeats Y 's strategy, a clone of X deterministically replaces Y . On the other hand, if Y 's strategy defeats X 's strategy, a clone of Y deterministically replaces X . (Stochastic or irrational replacement rules are also possible (Vandermeer and Yitbarek, 2012), as are scenarios in which a focal individual simultaneously interacts with all its neighbors during a time-step (Laird and Schamp, 2006, 2008; Rojas-Echenique and Allesina, 2011).) N time-steps are defined as one model generation. The models are run until strategy monoculture occurs, up to a maximum of 10^5 generations. There is no mutation, so once a monoculture is reached, no further changes to the node identities of the interaction graph are possible.

We consider values of Q between 0 and 1, inclusive, in increments of $1/100$, crossed with values of RI between 0 and 1, inclusive, in increments of $1/8, 1/14, 1/330, 1/385, 1/400$, and (again) $1/400$, for $s=6, 7, 20, 21, 100$, and 101 , respectively. (Where $1/8, 1/14, 1/330$, and $1/385$ are the smallest increments in RI for $s=6, 7, 20$, and 21 , respectively. The smallest increments for $s=100$ and $s=101$ are $1/41,650$ and $1/42,950$, respectively; however, in these cases, considering all possible values of RI would take an unfeasibly long simulation time.) For every value of RI considered, we start with a temporary s -strategy hierarchical tournament matrix and apply successive competitive reversals between randomly chosen pairs of strategies. If the matrix's RI value after the reversal is closer to the target value than it was before the reversal, the reversal is accepted. If the RI value becomes farther from the target value, the reversal is discarded. If the RI value remains equally close to the target value, the reversal is accepted with probability $1/2$ and discarded otherwise. The number of proposed reversals is 10^4 and 10^5 for smaller ($s \leq 21$) and larger ($s \geq 100$) numbers of strategies, respectively. This approach ensures that the target RI value is met (or approximated as closely as possible in cases where the target RI is not a multiple of ϕ) while still allowing the generation of random tournaments (whose unique manifestations outnumber the number of possible values of RI ; e.g., Laird and Schamp, 2009).

For every generation in every model run, we measure (i) current strategy richness, (ii) current strategy evenness, and (iii) current relative intransitivity. Current strategy richness, r , is simply the number of extant strategies. Current strategy evenness, $E_{\text{var}} \in [0, 1]$, is an index with high values (near 1) when strategies are approximately equally abundant and low values (near 0) when strategies have very different abundances. E_{var} is calculated as $1-(2/\pi)\arctan\{(\sum_i \ln(x_i) - \sum_j \ln(x_j))/r\}^2/r\}$, where x_i is the relative abundance of extant strategy i (Smith and Wilson, 1996). In community ecology, richness and evenness together traditionally represent the two components of diversity. Current relative intransitivity RI is calculated for modified tournament matrices that only include extant strategies. Additionally, for every model run we measure the number of generations until the first extinction.

3. Results and discussion

3.1. $k=4, 6$, or 8 neighbors per individual

For $k=4, 6$, and 8 , and $s=101$, the results were qualitatively similar. At low levels of quenched randomness, $Q < Q_c$ (where Q_c is approximately $0.41, 0.28$, and 0.27 for $k=4, 6$, and 8 , respectively; Table 1, Fig. A4), the number of strategies coexisting after 10^5 generations, r , was positively related to initial RI (Fig. 1, Fig. A3). This result is explicable in terms of the final RI on which assemblages settled, following earlier strategy extinctions. Regardless of the initial RI , the final RI of assemblages in which coexistence occurred was generally close to 1, although perfect intransitivity was by no means a prerequisite for strategy coexistence

² Coincidentally, this is also the number of strategies in D. Lovelace's *RPS-101*, "the most terrifyingly complex game ever" (<http://www.umop.com/rps101.htm>).

(Fig. 1, Fig. A3). High RI corresponds to situations where there is low variation in strategies' competitive abilities at the level of the assemblage, promoting strategy coexistence (Laird and Schamp,

2006). Further, sub-graphs of highly intransitive tournament graphs are themselves likely to be highly intransitive (e.g., Fig. A2; also see Section 2.3). Thus, it typically takes fewer strategy extinctions for an

Table 1

Critical quenched randomness, Q_c , for four numbers of neighbors per individual, k , and six initial numbers of strategies, s , as determined by the model output shown in Figs. A3 and A5 (population size: above dashed line: $N=62,500$; below dashed line: $N=10,000$). Q_c was estimated as the lowest value of Q for (and above) which more than 70% of the initial RI values examined resulted in monoculture within 10^5 generations. Note that for $k=3$, no critical quenched randomness is apparent, at least for these population sizes. See Fig. A4 for details.

Initial number of strategies, s	Critical quenched randomness, Q_c			
	$k=3$	$k=4$	$k=6$	$k=8$
6	NA	0.39	0.27	0.26
7	NA	0.41	0.27	0.26
20	NA	0.40	0.27	0.26
21	NA	0.41	0.27	0.26
100	NA	0.41	0.28	0.27
101	NA	0.41	0.28	0.27
101	NA	0.22	0.19	0.20

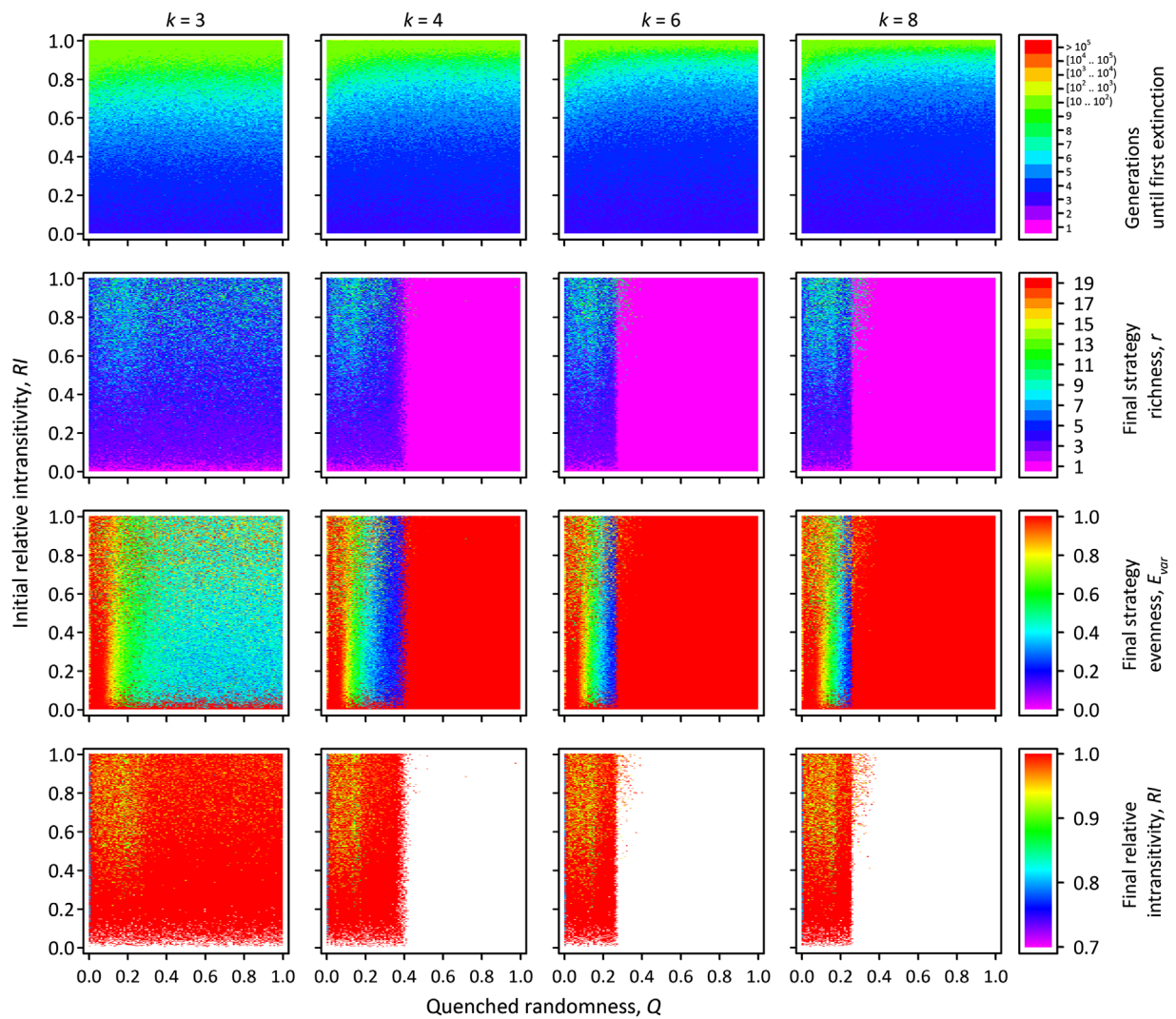


Fig. 1. Generations until first extinction (*top row*), final strategy richness (r ; *second row*), final strategy evenness (E_{var} ; *third row*), and final relative intransitivity (RI ; *bottom row*) as a function of the number of neighbors per individual (k ; *columns*), initial relative intransitivity (RI), and quenched randomness (Q). Population size: $N=62,500$; initial number of strategies: $s=101$. Each pixel represents a single model run. Interpretation of colors is given in the legends. (In the *bottom row*, white regions correspond to situations where $r < 3$, meaning that RI is undefined because $SS_{max}=SS_{min}$).

initially relatively intransitive assemblage to reach a state of intransitivity-mediated coexistence, compared to an initially relatively transitive assemblage. For a given initial strategy richness, assemblages with greater initial intransitivity therefore tend to have a greater final strategy richness.

This raises the question, then, of why the final strategy richness in even initially highly intransitive assemblages was less than 20 in all the model runs that started with $s=101$ strategies (Fig. 1, Table 2). That is, why do so many strategies go extinct so early in the simulations (Fig. A3)? This appears to be due to finite size effects associated with small average strategy population sizes in initially strategy-rich assemblages. Indeed, in model runs with $s=6, 7, 20,$ and 21 , the final strategy richness was often much closer to the maximum than in model runs with $s=100$ and 101 (Table 2, Fig. A3). Of course, the long-term number of strategies is capped at a maximum of s , so only limited inference can be drawn from this trend. To get at the issue more directly, we re-ran the $s=101$ model runs with a smaller interaction graph size of $N=10,000$, such that average strategy population sizes would be less than one sixth as large as in the original runs for a given number of extant strategies (Fig. A5). As expected, smaller interaction graphs typically supported fewer strategies in the long term compared to larger interaction graphs (Table 2, Fig. 2).

Due to the initial strategy extinctions, runs that started with odd numbers of strategies typically passed through their even counterparts quite rapidly, leading to the observation that there were only minor, inconsistent differences in the results within even-odd pairs of initial strategy richness (e.g., Tables 1 and 2; Fig. A3). An exception to this finding is in the low initial richness pair ($s=6$ versus 7) with maximum RI ; here, in the odd member of the pair, initial strategy extinctions often did not occur, leading to

greater long-term coexistence than in the even member of the pair (Table 2; Fig. A3).

A more interesting result is that regardless of the parity of the starting strategy richness, after 10^5 model generations the richness of the remaining strategies was almost always odd ($> 99.99\%$ across all combinations of $s, k, RI,$ and Q for $N=62,500$). Allesina and Levine (2011) demonstrated that in the absence of niche differences, tournaments conducted in a mean-field setting must collapse to an odd number of strategies, because “for any tournament composed of an even number of species, we can find a subtournament composed of an odd number of species that collectively wins against each of the remaining species more often than it loses, eventually driving the other species extinct” (p. 5640). This finding clearly generalizes to the network-structured populations examined here. On the other hand, real communities are rather less likely to be biased toward an odd number of strategies due to other, concurrent coexistence mechanisms such as niche differentiation, disturbance, trophic interactions, and source-sink dynamics.

When $Q > Q_c$, there was no longer a positive relationship between r and RI because long-term strategy coexistence was typically not possible (Fig. 1, Fig. A3). Rather, strategy monoculture generally occurred within 10^5 generations and typically much earlier (see time series in Fig. A3). Interestingly, Q_c appears to be largely independent of initial RI ; beyond Q_c , strategy monoculture was typical in both initially transitive and initially intransitive assemblages, although strategy coexistence was occasionally observed at values of Q slightly above Q_c in the latter case, especially on $k=6$ and $k=8$ interaction graphs (Fig. 1, Fig. A3). (Strategy monocultures also occurred when $Q < Q_c$, but only in very highly transitive assemblages.)

Table 2

Greatest observed strategy richness, r , after 10^5 generations, for four numbers of neighbors per individual, k , and six initial numbers of strategies, s . Population size: above dashed line: $N=62,500$; below dashed line: $N=10,000$.

Initial number of strategies, s	Greatest observed strategy richness, r			
	$k=3$	$k=4$	$k=6$	$k=8$
6	5	5	5	5
7	7	7	7	7
20	15	15	15	15
21	17	15	15	17
100	19	21	17	17
101	17	19	17	19
101	9	9	9	11

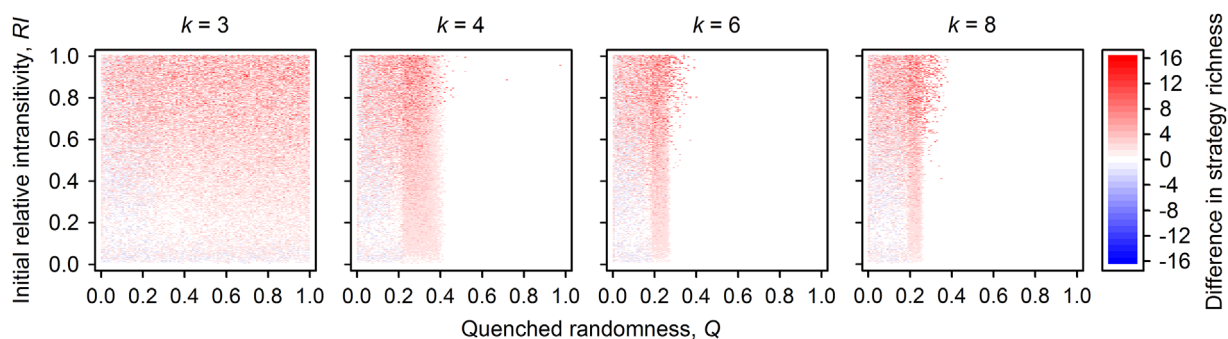


Fig. 2. Differences in final strategy richness between populations of $N=62,500$ and $N=10,000$ as a function of the number of neighbors per individual (k ; panels), initial relative intransitivity (RI), and quenched randomness (Q). Red regions indicate that the model run for $N=62,500$ had greater strategy richness after 10^5 model generations than the corresponding model run for $N=10,000$; blue regions indicate the model run for $N=10,000$ had the greater strategy richness; white regions indicate that the strategy richness was the same.

Why is there a cutoff of Q (Q_c), beyond which strategy coexistence is unlikely? Szabó et al. (2004) showed that for three-strategy tournaments, quenched randomness in the interaction graph is strongly positively related to the magnitude of strategy frequency oscillations, as evidenced by an increased area of the limit cycle relative to the total area of the phase space. If the amplitude of the oscillations becomes sufficiently large (i.e., when Q is greater than Q_c), monocultures are likely in finite populations (Fig. A6; bottom row). For instance, Fig. 3 shows three example time series for highly intransitive assemblages which initially had $s=101$ strategies, but which supported $r=3$ strategies in the long run ($k=4$, initial $RI=16/17$). As Q increases from 0.10 to 0.25 to 0.40, the magnitude of the oscillations of the three extant strategies increases and closely approaches the edges of the phase space. Indeed, in the full time-series for $Q=0.40$ (i.e., a value of Q very close to the estimated Q_c of 0.41; Table 1), one strategy came within a single individual of going extinct, a situation that, had it occurred, would have rapidly led to monoculture.

Unlike the effect of initial RI , within the region of strategy coexistence (i.e., $Q < Q_c$), Q had very little effect on final richness, except for values of Q very close to Q_c (Fig. 1, A3). On the other hand, Q had a sensitive influence, and initial RI only a weak one,

on the other component of strategy diversity, evenness (Fig. 1, A3). Specifically, final evenness was strongly negatively related to Q (except beyond Q_c , where monocultures prevail, and evenness was 1 by definition); however, initial RI was of little consequence to final evenness. As with richness, these evenness results can be interpreted in terms of the greater magnitude of strategy frequency oscillations as Q increases (Fig. 3). Larger oscillations mean that a small number of strategies typically dominate at any given time, while the rest have very low frequency; such disparity leads to reduced evenness (Smith and Wilson, 1996).

The number of generations until the first strategy extinction followed a somewhat different pattern from final richness, final evenness, and final RI , in that there was no evidence of an effect of a critical value of Q (Fig. 1, Fig. A3). Rather, there was a strong effect of initial RI , with more initially intransitive assemblages taking a longer time to lose their first strategy compared to initially transitive ones. When even the most weakly competing strategies can outcompete at least one of their competitors, and when even the most strongly competing strategies are outcompeted by at least one of their competitors, both of which frequently occur when RI approaches 1, it takes longer for the stronger competitors to purge the weak ones.

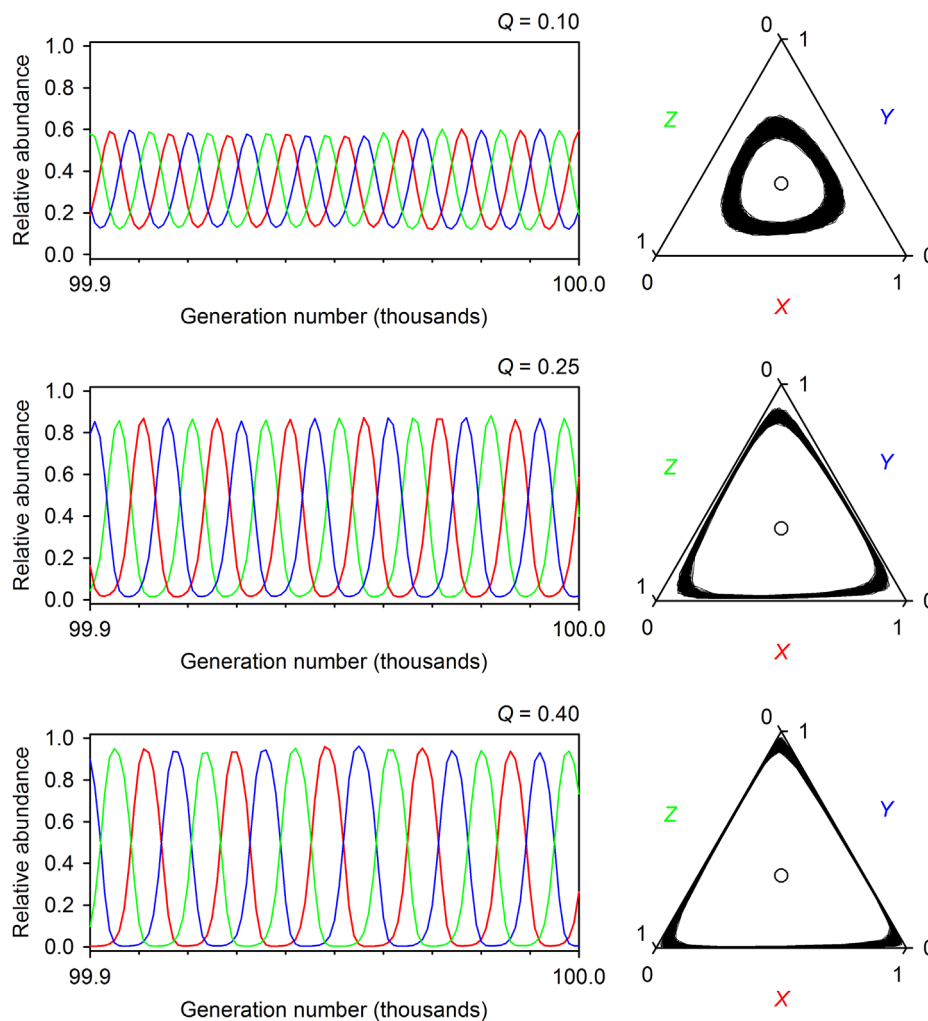


Fig. 3. Corresponding time series (generations 99,900 to 100,000; left column) and phase diagrams (generations 90,001 to 100,000; right column) for three example model runs for $N=62,500$, $k=4$, $s=101$, initial $RI=16/17$, and $Q=0.1$ (top row), 0.25 (middle row), or 0.4 (bottom row). Examples were chosen based on those that had the same final strategy richness (i.e., three strategies, arbitrarily labeled X (red), Y (blue), and Z (green) such that $X \rightarrow Y \rightarrow Z \rightarrow X$). Note that the model runs shown here are independent of those from the same parameter values in Fig. 1. In the phase diagrams, the point $(1/3, 1/3, 1/3)$ is shown for visual reference.

3.2. $k=3$ neighbors per individual

For $s=101$ and $k=3$, the results were qualitatively different from when individuals had $k=4, 6$, or 8 neighbors (Fig. 1, Fig. A3). Unlike those cases, when $k=3$ there was no apparent critical value of Q beyond which strategy coexistence was not possible (Table 1, Fig. A4). Although strategy frequency oscillations do increase with Q for $k=3$ (as with the other k -values), they fail to reach a magnitude that leads to strategy monoculture (e.g., Fig. A6; bottom row).

However, it is evident that these results are strongly dependent on population size. Our main results employed a population size of $N=62,500$. When contrasting three-strategy competition in perfectly intransitive tournaments with populations of $N=62,500$ and $N=10,000$, we see that the latter *do* have a value of Q beyond which monocultures sometimes occur (Fig. A6). Further, by observing the relationship between the magnitude of strategy frequency oscillations and population size in perfectly intransitive three-strategy tournaments played on regular random graphs ($Q=1$), we see that coexistence is less likely than monoculture when N is less than approximately 8876 (Fig. A7). Thus, it is clear that a consistently measurable Q_c for $k=3$ interaction graphs only comes into play at smaller population sizes than those examined in detail here.

Moreover, it is interesting to note that for all values of k , the magnitude of strategy frequency oscillations rose more rapidly with Q in $N=10,000$ populations than in $N=62,500$ populations (Fig. A6), leading to lower estimates of Q_c in the former (i.e., for $k=4, 6$, and 8 ; Table 1). Based on this trend, the $k=3$ results, and similar findings reported by Szabó and Fáth (2007), Szabó et al. (2004), Szolnoki and Szabó (2004), we surmise that Q_c may disappear altogether even for $k=4, 6$, or 8 in populations that are substantially greater than $N=62,500$. This is supported by further results given in Fig. A7, which show that when individuals have $k=4$ neighbors, three-strategy intransitive assemblages ($RI=1$) can be supported even in regular random graphs ($Q=1$), provided the population size is sufficiently high (N greater than approximately 206,297 for a predicted probability of strategy coexistence of > 0.5). The minimum population size, if there is one, that can sustain intransitive coexistence across all values of Q when $k=6$ or 8 is even larger (unknown, but greater than one million; Fig. A7).

3.3. Conclusions

Despite earlier misgivings surrounding its importance (Wilson, 1990), intransitive competition is now known to occur in many human endeavours (Arrow, 1950; Hughes, 1980; Kendall and Babington Smith, 1940; May, 1954; Riker, 1961; Tversky, 2004) and biological systems (Buss, 1980; Buss and Jackson, 1979; Dunstan and Johnson, 2005; Huisman and Weissing, 2001b; Kerr et al., 2002; Kirkup and Riley, 2004; Lankau and Strauss, 2007; Rubin, 1982; Sinervo and Lively, 1996; Sinervo et al., 2007; Taylor and Aarssen, 1990). In addition, attempts to understand population interaction structure and its effects on strategy dynamics and coexistence, particularly in cases where interaction connections are disordered and aspatial, have come to the fore (Du et al., 2009; Hadzibeganovic et al., 2012; Kuperman and Abramson, 2001; Lieberman et al., 2005; Lima et al., 2009; Nowak, 2006; Pacheco et al., 2006; Perc et al., 2013; Szabó et al., 2004; Szolnoki and Szabó, 2004; Szolnoki and Perc, 2009; Szolnoki et al., 2008; Wang et al., 2006; Ying et al., 2007).

Here, we link these two aspects of evolutionary game theory and evolutionary graph theory to show how relative intransitivity and quenched randomness in small-world networks interact to determine strategy coexistence in finite populations. In most cases

in our models, when quenched randomness is relatively low, greater initial intransitivity leads to greater long-term coexistence because it takes fewer extinctions to attain a highly intransitive state in which the competitive abilities of strategies are balanced at the community level. However, when quenched randomness exceeds a critical value, Q_c , population fluctuations increase to such a degree that coexistence is no longer possible, and a single strategy typically takes over the entire network. This emphasizes the importance of space per se in determining intransitivity-mediated strategy coexistence (e.g., Durrett and Levin, 1998; Frean and Abraham, 2001; Kerr et al., 2002; Laird, 2014) and reaffirms the notion that dispersal and long-range connections can potentially destroy coexistence by synchronizing regions of networks that would otherwise evolve independently (Szabó et al., 2004).

We further show that Q_c depends positively on the number of interacting individuals in the system, and that this critical value can even disappear in populations that are sufficiently large (where “sufficiently large” itself depends on neighborhood size, k). We nevertheless argue that quenched randomness and long-range connections are still likely to be relevant to the maintenance of diversity in many intransitive systems, particularly those of a social or biological nature. Our argument stems from the characteristic size of typical socio-biological systems, as compared to physical ones: In statistical physics, a critical aspect of simulation-model building is ensuring that the system is large enough to avoid accidental extinctions associated with finite-size effects (e.g., Szabó et al., 2004). This makes good sense when dealing with multitudinous interacting particles, for example. However, in community ecology, the main focus of our work here, populations are finite in practice, and, indeed, often small. Thus, we contend that it is important to understand the nature of Q_c on the coexistence of strategies in intransitively competing systems, even if this critical value vanishes as population size approaches infinity. Just as finite populations are important to our understanding of the evolutionary game dynamics of cooperation (Nowak et al., 2004; Taylor et al., 2007; Traulsen et al., 2005), so too are finite populations important to our understanding of the coexistence criteria for intransitively competing strategies.

Our results lend support to the hypothesis that intransitivity-mediated coexistence may be most prevalent in spatial systems whose high natural clustering (‘cliquishness’) and characteristic path-lengths (‘degrees of separation’; Watts and Strogatz, 1998) hinder the spontaneous emergence of global oscillations and guard against the collapse of diversity. It is therefore intriguing, and worthy of additional study, that several of the best examples of this potential mechanism of coexistence come from systems where competition and dispersal/colony growth are predominantly local in their extent (e.g., Jackson and Buss, 1975; Kerr et al., 2002). On the other side of this argument, it is tempting to speculate that ongoing transitions toward socially structured networks with very long distance connections may lead to the erosion of intransitive preferences (at the network level) in humans, and possibly the loss of ideological or cultural diversity—a process that may be mitigated or enhanced, respectively, as the size of the networks (N) or the size of neighborhoods (k) expands.

Our results also suggest several other outstanding questions. For example, how do intransitivity and quenched randomness affect strategy coexistence when competition is more symmetrical, such that the outcome of an individual competitive interaction is uncertain (Vandermeer and Yitbarek, 2012)? What is the effect when the interaction graph is not static, but free to evolve as connections are severed, shuffled, and re-established (Pacheco et al., 2006; Santos et al., 2006; Szolnoki and Perc, 2009)? Does annealed randomness produce similar results to quenched

randomness, as it does in three-strategy intransitive assemblages (Szabó et al., 2004)? While these questions are as yet unanswered, it is certainly clear that variation in interaction graph topology is a crucial aspect of whether intransitivity-mediated coexistence can be realized in systems playing rock–paper–scissors and its more strategy-rich counterparts.

Acknowledgments

We gratefully acknowledge E. Bonderover, L. Chang, P. Leventis, and S. Yazdani for technical assistance. We thank our editor and anonymous referees for their constructive comments. This research was funded by the Natural Science and Engineering Research Council of Canada and the University of Lethbridge Research Fund.

Appendix A. Supporting information

Supplementary data associated with this article can be found in the online version at <http://dx.doi.org/10.1016/j.jtbi.2014.10.010>.

References

- Allesina, S., Levine, J.M., 2011. A competitive network theory of species diversity. *Proc. Natl. Acad. Sci. U.S.A.* 108, 5638–5642.
- Arrow, K.J., 1950. A difficulty in the concept of social welfare. *J. Pol. Econ.* 58, 328–346.
- Bezembinder, T.G.G., 1981. Circularity and consistency in paired comparisons. *Br. J. Math. Stat. Psychol.* 34, 16–37.
- Bleay, C., Comendant, T., Sinervo, B., 2007. An experimental test of frequency-dependent selection on male mating strategy in the field. *Proc. R. Soc. B: Biol. Sci.* 274, 2019–2025.
- Buss, L.W., 1976. Better living through chemistry: The relationship between allelochemical interactions and competitive networks. In: Harrison, F.W., Cowden, R.R. (Eds.), *Aspects of Sponge Biology*. Academic Press, New York, NY, pp. 315–328.
- Buss, L.W., 1980. Competitive intransitivity and size–frequency distributions of interacting populations. *Proc. Natl. Acad. Sci. U.S.A.* 77, 5355–5359.
- Buss, L.W., Jackson, J.B.C., 1979. Competitive networks: nontransitive competitive relationships in cryptic coral reef environments. *Am. Nat.* 113, 223–234.
- Chesson, P., 2000. Mechanisms of species diversity. *Annu. Rev. Ecol. Syst.* 31, 343–366.
- Czárán, T., Hoekstra, R.F., Paige, L., 2002. Chemical warfare between microbes promotes biodiversity. *Proc. Natl. Acad. Sci. U.S.A.* 99, 786–790.
- Du, W.-B., Cao, X.-B., Hu, M.-B., Wang, W.-X., 2009. Asymmetric cost in snowdrift game on scale-free networks. *EPL*, 60004.
- Dunstan, P.K., Johnson, C.R., 2005. Predicting global dynamics from local interactions: individual-based models predict complex features of marine epibenthic communities. *Ecol. Model.* 186, 221–233.
- Durrett, R., Levin, S.A., 1994. Stochastic spatial models: a user's guide to ecological applications. *Philos. Trans. R. Soc. London, Ser. B* 343, 329–350.
- Durrett, R., Levin, S.A., 1998. Spatial aspects of interspecific competition. *Theor. Popul. Biol.* 53, 30–43.
- Frean, M., Abraham, E.R., 2001. Rock–scissors–paper and the survival of the weakest. *Proc. R. Soc. B: Biol. Sci.* 268, 1323–1327.
- Gilpin, M.E., 1975. Limit cycles in competition communities. *Am. Nat.* 109, 51–60.
- Hadzibeganovic, T., Lima, F.W.S., Stauffer, D., 2012. Evolution of tag-mediated altruistic behavior in one-shot encounters on large-scale complex networks. *Comput. Phys. Commun.* 183, 2315–2321.
- Hauert, C., 2001. Fundamental clusters in spatial 2×2 games. *Proc. R. Soc. B: Biol. Sci.* 268, 761–769.
- Hauert, C., 2002. Effects of space in 2×2 games. *Int. J. Bifurcation Chaos* 12, 1531–1548.
- Hauert, C., 2006. Spatial effects in social dilemmas. *J. Theor. Biol.* 240, 627–636.
- Hauert, C., Doebeli, M., 2004. Spatial structure often inhibits the evolution of cooperation in the snowdrift game. *Nature* 428, 643–646.
- Hofbauer, J., Sigmund, K., 1998. *Evolutionary Games and Population dynamics*. Cambridge University Press, Cambridge.
- Hughes, R.I.G., 1980. Rationality and intransitive preferences. *Analysis* 40, 132–134.
- Huisman, J., Weissing, F.J., 1999. Biodiversity of plankton by species oscillations and chaos. *Nature* 402, 407–410.
- Huisman, J., Weissing, F.J., 2001a. Fundamental unpredictability in multispecies competition. *Am. Nat.* 157, 488–494.
- Huisman, J., Weissing, F.J., 2001b. Biological conditions for oscillations and chaos generated by multispecies competition. *Ecology* 82, 2682–2695.
- Huisman, J., Johansson, A.M., Folmer, E.O., Weissing, F.J., 2001. Towards a solution of the plankton paradox: the importance of physiology and life history. *Ecol. Lett.* 4, 408–411.
- Huston, M.A., 1994. *Biological Diversity: The Coexistence of Species on Changing Landscapes*. Cambridge University Press, Cambridge.
- Hutchinson, G.E., 1959. Homage to Santa Rosalia or Why are there so many kinds of animals? *Am. Nat.* 93, 145–159.
- Jackson, J.B.C., Buss, L.W., 1975. Allelopathy and spatial competition among coral reef invertebrates. *Proc. Natl. Acad. Sci. U.S.A.* 72, 5160–5163.
- Karlson, R.H., Jackson, J.B.C., 1981. Competitive networks and community structure – a simulation study. *Ecology* 62, 670–678.
- Károlyi, G., Neufeld, Z., Scheuring, I., 2005. Rock–scissors–paper game in a chaotic flow: the effect of dispersion on the cyclic competition of microorganisms. *J. Theor. Biol.* 236, 12–20.
- Kendall, M.G., Babington Smith, B., 1940. On the method of paired comparisons. *Biometrika* 31, 324–345.
- Kerr, B., Riley, M.A., Feldman, M.W., Bohannan, B.J.M., 2002. Local dispersal promotes biodiversity in a real-life game of rock–paper–scissors. *Nature* 418, 171–174.
- Kirkup, B.C., Riley, M.A., 2004. Antibiotic-mediated antagonism leads to a game of rock–paper–scissors in vivo. *Nature* 428, 412–414.
- Kuperman, M., Abramson, G., 2001. Small world effect in an epidemiological model. *Phys. Rev. Lett.* 86, 2909–2912.
- Laird, R.A., 2011. Green-beard effect predicts the evolution of traitorousness in the two-tag Prisoner's Dilemma. *J. Theor. Biol.* 288, 84–91.
- Laird, R.A., 2012. Evolutionary strategy dynamics for tag-based cooperation and defection in the spatial and aspatial snowdrift game. *Int. J. Bifurcation Chaos* 22, 1230039.
- Laird, R.A., 2013. Static cooperator-defector patterns in models of the snowdrift game played on cycle graphs. *Phys. Rev. E: Stat. Nonlinear Soft Matter Phys.* 88, 012105.
- Laird, R.A., 2014. Population interaction structure and the coexistence of bacterial strains playing 'rock–paper–scissors'. *Oikos* 123, 472–480.
- Laird, R.A., Schamp, B.S., 2006. Competitive intransitivity promotes species coexistence. *Am. Nat.* 168, 182–193.
- Laird, R.A., Schamp, B.S., 2008. Does local competition increase the coexistence of species in intransitive networks? *Ecology* 89, 237–247.
- Laird, R.A., Schamp, B.S., 2009. Species coexistence, intransitivity, and topological variation in competitive tournaments. *J. Theor. Biol.* 256, 90–95.
- Laird, R.A., Goyal, D., Yazdani, S., 2013. Geometry of 'standoffs' in lattice models of the spatial Prisoner's Dilemma and Snowdrift games. *Physica A* 392, 3622–3633.
- Lankau, R.A., Strauss, S.Y., 2007. Mutual feedbacks maintain both genetic and species diversity in a plant community. *Science* 317, 1561–1563.
- Lieberman, E., Hauert, C., Nowak, M.A., 2005. Evolutionary dynamics on graphs. *Nature* 433, 312–316.
- Lima, F.W.S., Hadzibeganovic, T., Stauffer, D., 2009. Evolution of ethnocentrism on undirected and directed Barbási-Albert networks. *Physica A* 388, 4999–5004.
- May, K.O., 1954. Intransitivity, utility, and the aggregation of preference patterns. *Econometrica* 22, 1–13.
- May, R.M., Leonard, W.J., 1975. Nonlinear aspects of competition between three species. *SIAM J. Appl. Math.* 29, 243–253.
- Maynard Smith, J., 1982. *Evolution and the Theory of Games*. Cambridge University Press, Cambridge, UK.
- Nahum, J.R., Harding, B.N., Kerr, B., 2011. Evolution of restraint in a structured rock–paper–scissors community. *Proc. Natl. Acad. Sci. U.S.A.* 108, 10831–10838.
- Neumann, G., Schuster, S., 2007. Continuous model for the rock–scissors–paper game between bacteriocin producing bacteria. *J. Math. Biol.* 54, 815–846.
- Nowak, M.A., 2006. *Evolutionary Dynamics: Exploring the Equations of Life*. Harvard University Press, Cambridge.
- Nowak, M.A., May, R.M., 1992. Evolutionary games and spatial chaos. *Nature* 359, 826–829.
- Nowak, M.A., May, R.M., 1993. The spatial dilemmas of evolution. *Int. J. Bifurcation Chaos* 3, 35–78.
- Nowak, M.A., Bonhoeffer, S., May, R.M., 1994a. More spatial games. *Int. J. Bifurcation Chaos* 4, 33–56.
- Nowak, M.A., Bonhoeffer, S., May, R.M., 1994b. Spatial games and the maintenance of cooperation. *Proc. Natl. Acad. Sci. U.S.A.* 91, 4877–4881.
- Nowak, M.A., Sasaki, A., Taylor, C., Fudenberg, D., 2004. Emergence of cooperation and evolutionary stability in finite populations. *Nature* 428, 646–650.
- Pacheco, J.M., Traulsen, A., Nowak, M.A., 2006. Co-evolution of strategy and structure in complex networks with dynamical linking. *Phys. Rev. Lett.* 97, 258103.
- Paquin, C.E., Adams, J., 1983. Relative fitness can decrease in evolving population of *S. cerevisiae*. *Nature* 306, 368–371.
- Perc, M., Gómez-Gardeñes, J., Szolnoki, A., Flórida, L.M., Moreno, Y., 2013. Evolutionary dynamics of group interactions on structured populations: a review. *J. R. Soc. Interface* 10, 20120997.
- Petratits, P.S., 1979. Competitive networks and measures of intransitivity. *Am. Nat.* 114, 921–925.
- Reichenbach, T., Mobilia, M., Frey, E., 2007. Mobility promotes and jeopardizes biodiversity in rock–paper–scissors games. *Nature* 448, 1046–1049.
- Riker, W.H., 1961. Voting and the summation of preferences: an interpretive bibliographic review of selected developments during the last decade. *Am. Pol. Sci. Rev.* 55, 900–911.
- Rojas-Echenique, J., Allesina, S., 2011. Interaction rules affect species coexistence in intransitive networks. *Ecology* 92, 1174–1180.

- Rubin, J.A., 1982. The degree of intransitivity and its measurement in an assemblage of encrusting cheilostome bryozoa. *J. Exp. Mar. Biol. Ecol.* 60, 119–128.
- Santos, F.C., Pacheco, J.M., Lenaerts, T., 2006. Cooperation prevails when individuals adjust their social ties. *PLoS Comput. Biol.* 2, 1284–1291.
- Schreiber, S.J., Killingback, T., 2013. Spatial heterogeneity promotes coexistence of rock–paper–scissors metacommunities. *Theor. Popul. Biol.* 86, 1–11.
- Sigmund, K., 2010. *The Calculus of Selfishness*. Princeton University Press, Princeton.
- Sinervo, B., Lively, C.M., 1996. The rock–paper–scissors game and the evolution of alternative male strategies. *Nature* 380, 240–243.
- Sinervo, B., Heulin, B., Surget-Groba, Y., Clobert, J., Miles, D.B., Corl, A., Chaine, A., Davis, A., 2007. Models of density-dependent genic selection and a new rock–paper–scissors social system. *Am. Nat.* 170, 663–680.
- Slater, P., 1961. Inconsistencies in a schedule of paired comparisons. *Biometrika* 48, 303–312.
- Smith, B., Wilson, J.B., 1996. A consumer's guide to evenness indices. *Oikos* 76, 70–82.
- Szabó, G., Tóke, C., 1998. Evolutionary prisoner's dilemma game on a square lattice. *Phys. Rev. E: Stat. Phys. Plasmas Fluids Relat. Interdisciplin. Top.* 58, 69–73.
- Szabó, G., Fáth, G., 2007. Evolutionary games on graphs. *Phys. Rep.* 446, 97–216.
- Szabó, G., Szolnoki, A., Izsák, R., 2004. Rock–scissors–paper game on regular small-world networks. *J. Phys. A: Math. Gen.* 37, 2599–2609.
- Szolnoki, A., Szabó, G., 2004. Phase transitions for rock–scissors–paper game on different networks. *Phys. Rev. E: Stat. Nonlinear Soft Matter Phys.* 70, 037102.
- Szolnoki, A., Perc, M., 2009. Resolving social dilemmas on evolving random networks. *EPL* 86, 30007.
- Szolnoki, A., Perc, M., Szabó, G., 2008. Diversity of reproduction rate supports cooperation in the prisoner's dilemma game on complex networks. *Eur. Phys. J. B* 61, 505–509.
- Tainaka, K.-i., 1988. Lattice model for the Lotka–Volterra system. *J. Phys. Soc. Jpn.* 57, 2588–2590.
- Tainaka, K.-i., 2001. Physics and ecology of rock–paper–scissors game. *Lect. Notes Comput. Sci* 2063, 384–395.
- Taylor, D.R., Aarssen, L.W., 1990. Complex competitive relationships among genotypes of three perennial grasses: Implications for species coexistence. *Am. Nat.* 136, 305–327.
- Taylor, P.D., Day, T., Wild, G., 2007. Evolution of cooperation in a finite homogeneous graph. *Nature* 447, 469–472.
- Tokeshi, M., 1999. *Species Coexistence: Ecological and Evolutionary Perspectives*. Blackwell Science, Oxford.
- Traulsen, A., Claussen, J.C., Hauert, C., 2005. Coevolutionary dynamics: from finite to infinite populations. *Phys. Rev. Lett.* 95, 238701.
- Tversky, 2004. Intransitivity of preferences. In: Shafir, E. (Ed.), *Preference, Belief, and Similarity: Selected Writings*. Amos Tversky. MIT Press, Cambridge, MA, pp. 433–461.
- Vandermeer, J., 2011. Intransitive loops in ecosystem models: from stable foci to heteroclinic cycles. *Ecol. Complexity* 8, 92–97.
- Vandermeer, J., Yitbarek, S., 2012. Self-organized spatial pattern determines biodiversity in spatial competition. *J. Theor. Biol.* 300, 48–56.
- Vukov, J., Szolnoki, A., Szabó, G., 2013. Diverging fluctuations in a spatial five-species cyclic dominance game. *Phys. Rev. E: Stat. Nonlinear Soft Matter Phys.* 88, 022123.
- Wang, W.-X., Ren, J., Chen, G., Wang, B.-H., 2006. Memory-based snowdrift game on networks. *Phys. Rev. E: Stat. Nonlinear Soft Matter Phys.* 74, 056113.
- Watts, D.J., Strogatz, S.H., 1998. Collective dynamics of 'small-world' networks. *Nature* 393, 440–442.
- Wilson, J.B., 1990. Mechanisms of species coexistence: twelve explanations for Hutchinson's 'Paradox of the Plankton': evidence from New Zealand plant communities. *N.Z. J. Ecol.* 13, 17–42.
- Wilson, J.B., 2011. The twelve theories of co-existence in plant communities: the doubtful, the important, and the unexplored. *J. Veg. Sci.* 22, 184–195.
- Wootton, J.T., 2001. Local interactions predict large-scale pattern in empirically derived cellular automata. *Nature* 413, 841–844.
- Ying, C.-y., Hua, D.-y., Wang, L.-y., 2007. Phase transitions for a rock–paper–scissors model with long-range-directed interactions. *J. Phys. A: Math. Theor.* 40, 4477–4482.
- Zhang, G.-Y., Chen, Y., Qi, W.-K., Qing, S.-M., 2009. Four-state rock–paper–scissors games in constrained Newman–Watts networks. *Phys. Rev. E: Stat. Nonlinear Soft Matter Phys.* 79, 062901.

Appendix A. Supplementary data

Competitive intransitivity, population interaction structure, and strategy coexistence

Robert A. Laird^{a,*}, Brandon S. Schamp^b

^a *Department of Biological Sciences, University of Lethbridge, Lethbridge, AB T1K 3M4, Canada*

^b *Department of Biology, Algoma University, Sault Ste. Marie, ON P6A 2G3, Canada*

* Corresponding author. *E-mail address:* robert.laird@uleth.ca

Contents

Page numbers are hyperlinked to figures (click on red numbers).

Fig. A1. An example of a regular 25-individual interaction graph	2
Fig. A2. An example of a maximally intransitive seven-strategy tournament	4
Fig. A3. Full model results for $k = 3, 4, 6,$ and $8,$ and $s = 6, 7, 20, 21, 100,$ and 101	9
Fig. A4. Estimation of Q_c	34
Fig. A5. Model results for $s = 101$ on the $N = 10000$ interaction graph	36
Fig. A6. Magnitude of population fluctuations in intransitive three-strategy assemblages of varying quenched randomness	38
Fig. A7. Magnitude of population fluctuations in intransitive three-strategy assemblages of varying numbers of individuals	40

Fig. A1. [Subsequent page]. An example of a regular 25-individual interaction graph. Nodes (circles, labeled A-Y) represent individuals, and edges (black, solid lines) connect individuals that interact. $N = 25$ nodes; $k = 4$ edges per node. $Q = 0.1$ meaning that $QNk/2 = 5$ random connections in the original lattice are severed (i.e., *AU*, *DE*, *JO*, *MN*, and *QR*; dashed grey lines), and the resulting half-edges are randomly joined (i.e., *AQ*, *DJ*, *EM*, *NR*, *OU*). While this example has $N = 25$ nodes, most of our actual simulations have $N = 62500$ nodes.

Fig. A1

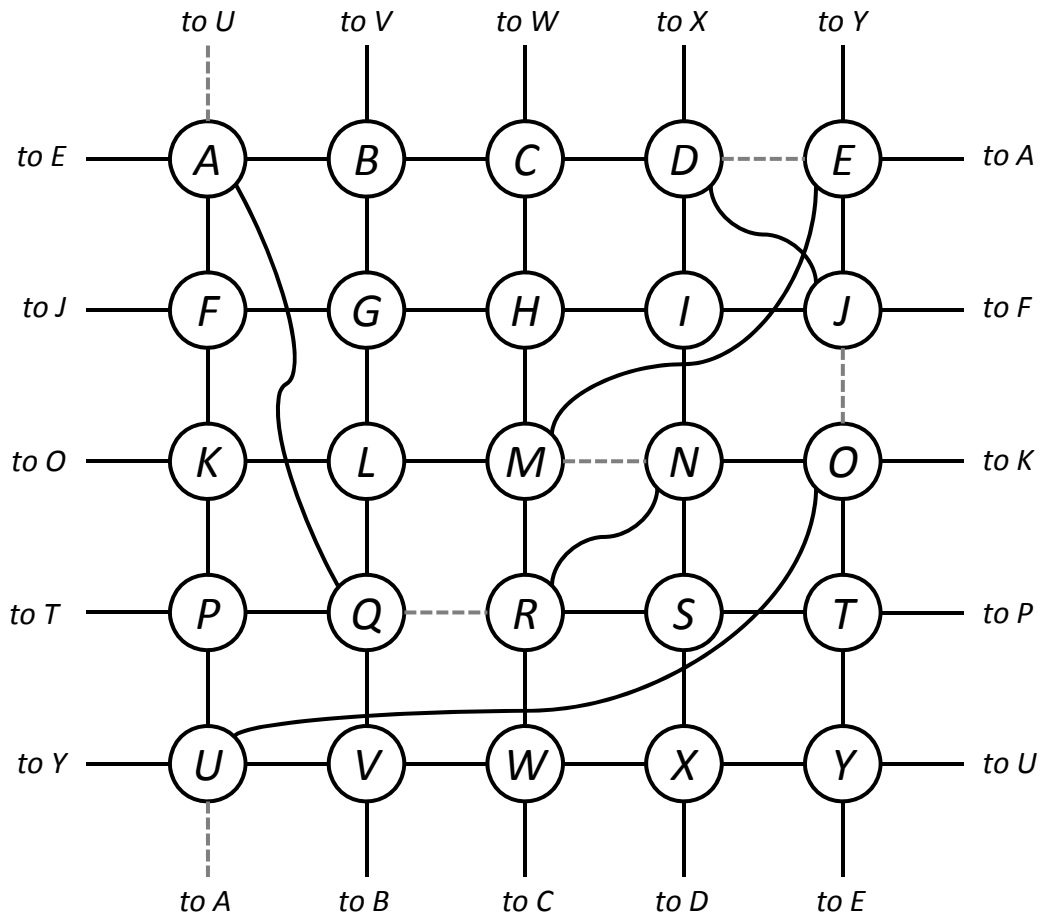


Fig. A2. [Subsequent four pages]. *Matrices:* An example $s = 7$ -strategy tournament matrix ($M = [m_{ij}]$) of maximum intransitivity ($RI = 1$). Strategies are labeled 1-7. When $m_{ij} = 1$, the strategy of row i outcompetes the strategy of column j . When $m_{ij} = 0$, the strategy of row i is outcompeted by the strategy of column j (or nothing happens in the case of $i = j$). The column marked w gives the row sums, the number of wins each strategy has against the other strategies; taken together, the w column represents the score sequence of the tournament. *Graphs:* The graphs all correspond to M . The graph in the blue box is uncolored; the other graphs are colored to highlight each sub-graph triad in turn (of which there is a total of $C(s, 3) = 35$). In each case, nodes represent strategies and directed edges represent the competitive relationships within a pair of strategies, with $X \rightarrow Y$ indicating that strategy Y outcompetes strategy X . Note that this is the opposite direction of directed edges in some previous studies; however, this formulation is intuitive because it means that arrows flow in the direction of competitive replacement. In the graphs that highlight the triads, intransitive triads are given in green and transitive triads are given in red. Note that there are exactly $\phi^{-1} = (s^3 - s)/24 = 14$ intransitive triads in this maximally intransitive tournament, as demonstrated by Kendall and Babington Smith (1940).

Fig. A2
Part 1 of 4

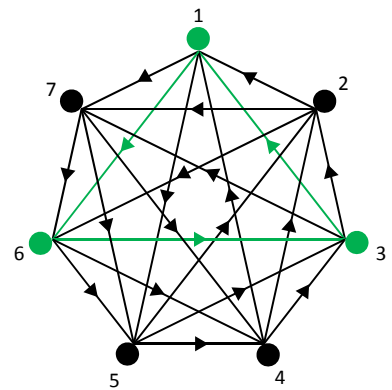
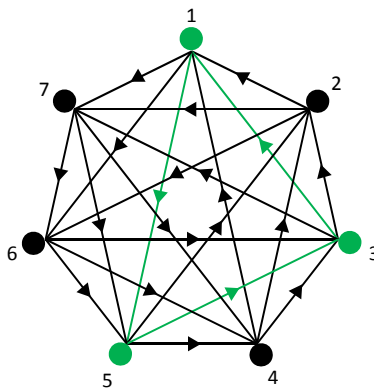
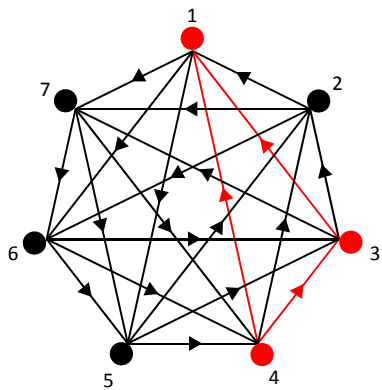
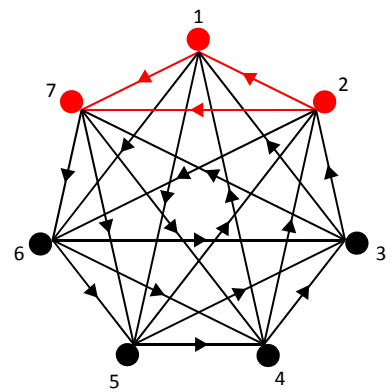
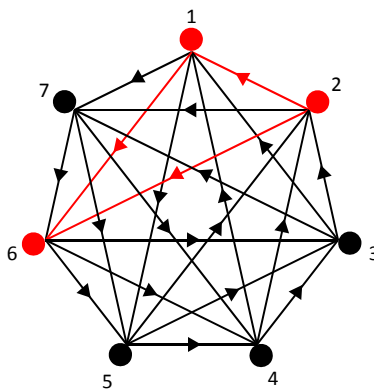
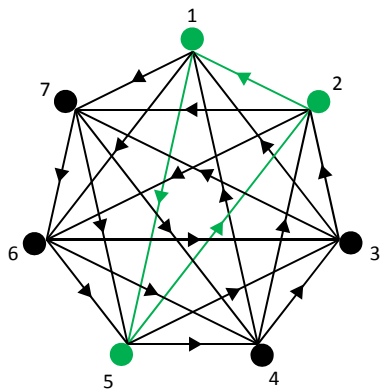
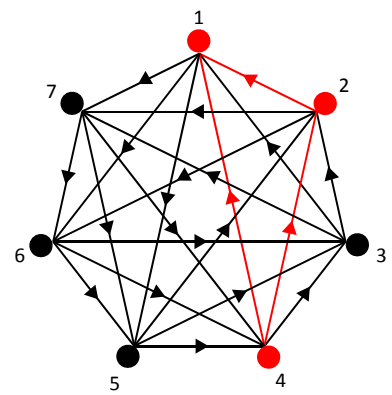
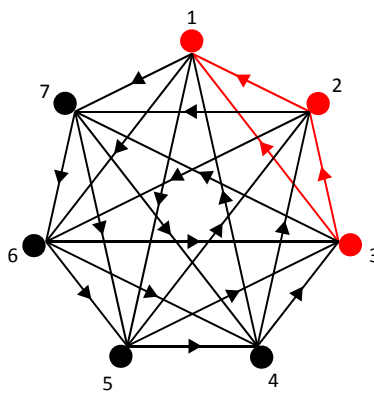
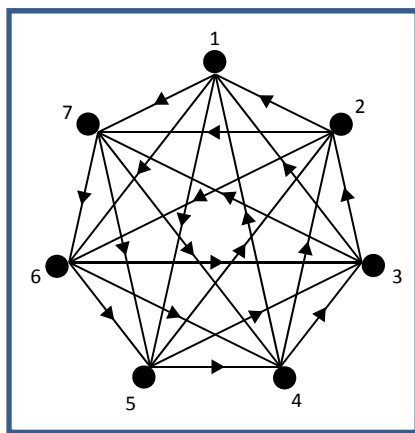
$$M = \begin{array}{c|cccccccc} & 1 & 2 & 3 & 4 & 5 & 6 & 7 & w \\ \hline 1 & 0 & 1 & 1 & 1 & 0 & 0 & 0 & 3 \\ 2 & 0 & 0 & 1 & 1 & 1 & 0 & 0 & 3 \\ 3 & 0 & 0 & 0 & 1 & 1 & 1 & 0 & 3 \\ 4 & 0 & 0 & 0 & 0 & 1 & 1 & 1 & 3 \\ 5 & 1 & 0 & 0 & 0 & 0 & 1 & 1 & 3 \\ 6 & 1 & 1 & 0 & 0 & 0 & 0 & 1 & 3 \\ 7 & 1 & 1 & 1 & 0 & 0 & 0 & 0 & 3 \end{array}$$


Fig. A2
Part 2 of 4

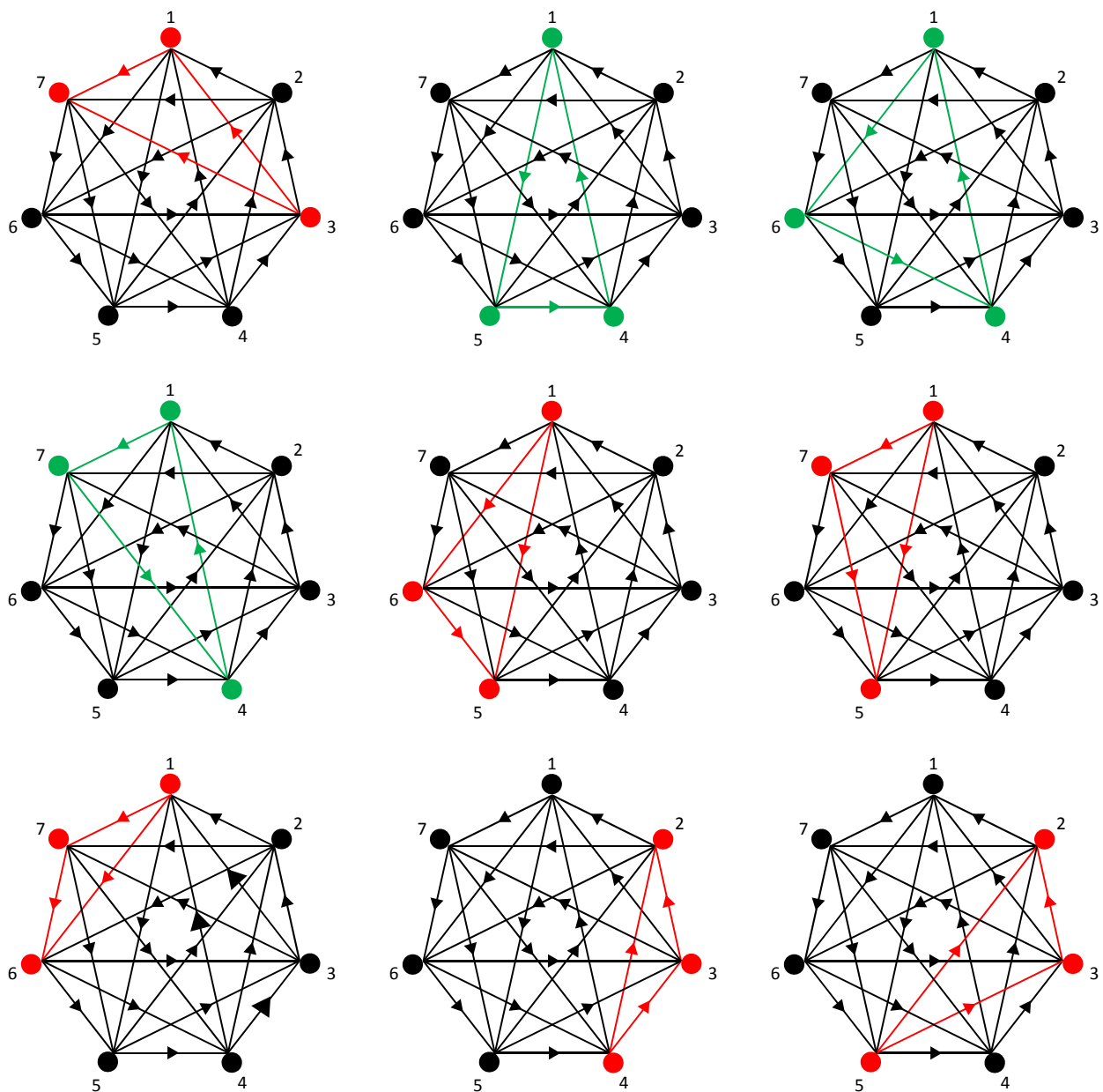
$$M = \begin{array}{c|ccccccc|c} & 1 & 2 & 3 & 4 & 5 & 6 & 7 & w \\ \hline 1 & 0 & 1 & 1 & 1 & 0 & 0 & 0 & 3 \\ 2 & 0 & 0 & 1 & 1 & 1 & 0 & 0 & 3 \\ 3 & 0 & 0 & 0 & 1 & 1 & 1 & 0 & 3 \\ 4 & 0 & 0 & 0 & 0 & 1 & 1 & 1 & 3 \\ 5 & 1 & 0 & 0 & 0 & 0 & 1 & 1 & 3 \\ 6 & 1 & 1 & 0 & 0 & 0 & 0 & 1 & 3 \\ 7 & 1 & 1 & 1 & 0 & 0 & 0 & 0 & 3 \end{array}$$


Fig. A2
Part 3 of 4

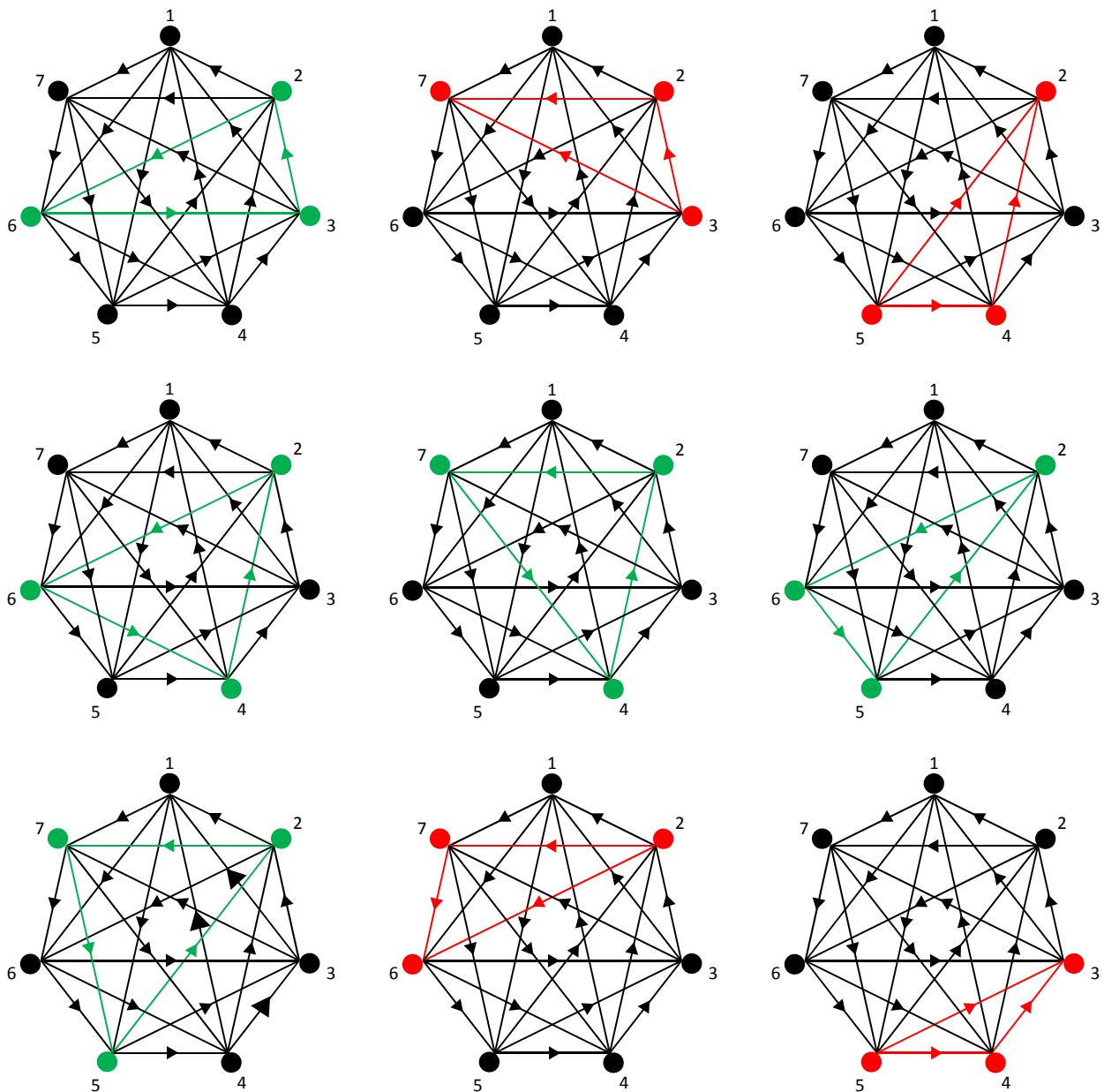
$$M = \begin{array}{c|cccccccc} & 1 & 2 & 3 & 4 & 5 & 6 & 7 & w \\ \hline 1 & 0 & 1 & 1 & 1 & 0 & 0 & 0 & 3 \\ 2 & 0 & 0 & 1 & 1 & 1 & 0 & 0 & 3 \\ 3 & 0 & 0 & 0 & 1 & 1 & 1 & 0 & 3 \\ 4 & 0 & 0 & 0 & 0 & 1 & 1 & 1 & 3 \\ 5 & 1 & 0 & 0 & 0 & 0 & 1 & 1 & 3 \\ 6 & 1 & 1 & 0 & 0 & 0 & 0 & 1 & 3 \\ 7 & 1 & 1 & 1 & 0 & 0 & 0 & 0 & 3 \end{array}$$


Fig. A2
Part 4 of 4

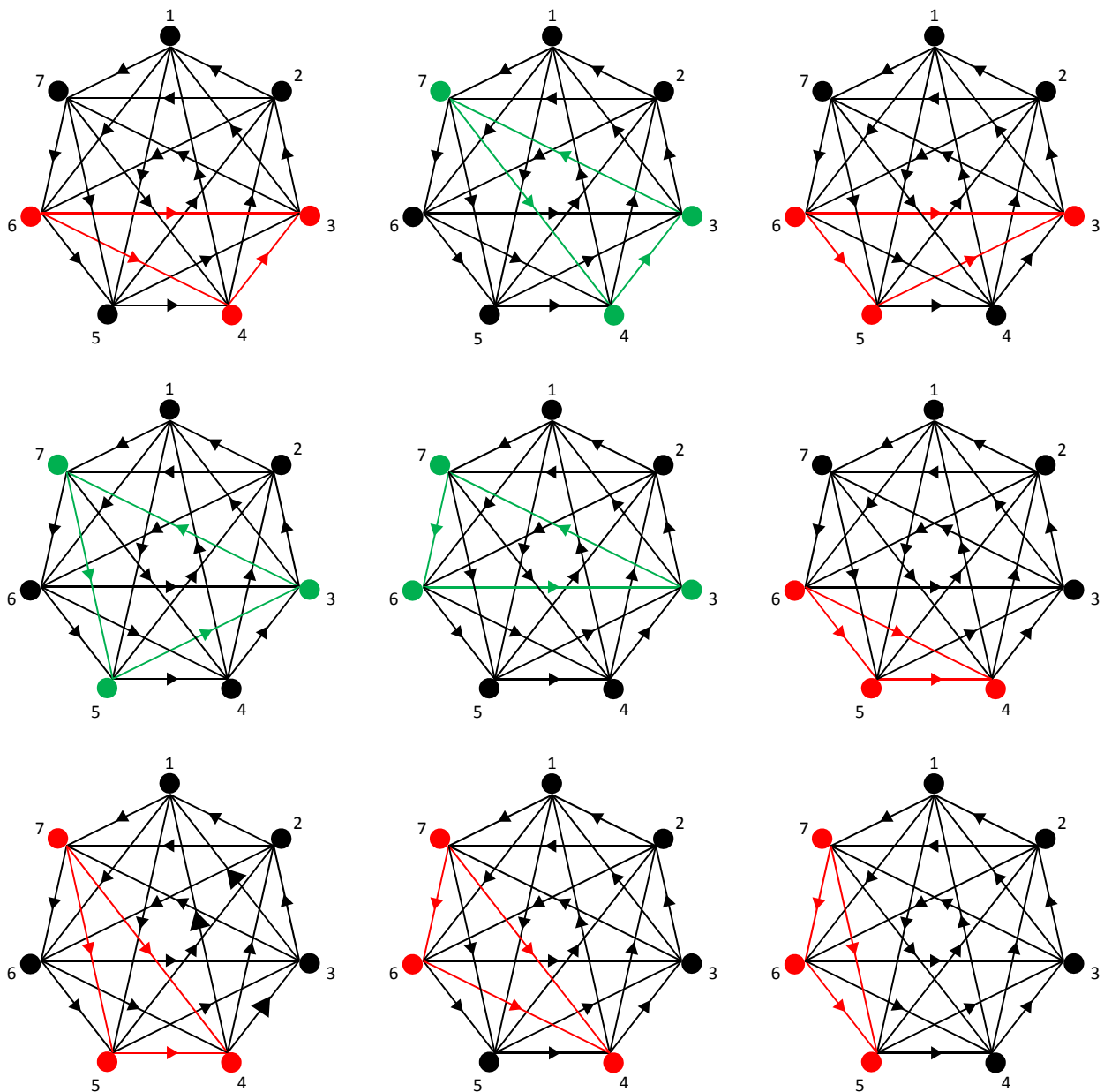
$$M = \begin{array}{c|ccccccc|c} & 1 & 2 & 3 & 4 & 5 & 6 & 7 & w \\ \hline 1 & 0 & 1 & 1 & 1 & 0 & 0 & 0 & 3 \\ 2 & 0 & 0 & 1 & 1 & 1 & 0 & 0 & 3 \\ 3 & 0 & 0 & 0 & 1 & 1 & 1 & 0 & 3 \\ 4 & 0 & 0 & 0 & 0 & 1 & 1 & 1 & 3 \\ 5 & 1 & 0 & 0 & 0 & 0 & 1 & 1 & 3 \\ 6 & 1 & 1 & 0 & 0 & 0 & 0 & 1 & 3 \\ 7 & 1 & 1 & 1 & 0 & 0 & 0 & 0 & 3 \\ \hline \end{array}$$


Fig. A3. [Subsequent 24 pages]. Each sub-figure, (a) through (x), shows the full model results (when $N = 62500$) for a particular combination of the number of neighbours per individual (i.e., the number of edges per node; k) and the initial number of strategies (s), as given in the following hyperlinked table (click on red letters):

Initial number of strategies (s)	Neighbours per individual (k)			
	3	4	6	8
6	(a)	(g)	(m)	(s)
7	(b)	(h)	(n)	(t)
20	(c)	(i)	(o)	(u)
21	(d)	(j)	(p)	(v)
100	(e)	(k)	(q)	(w)
101	(f)	(l)	(r)	(x)

In each sub-figure, the *top row* (composed of a single panel) gives the number of generations until the first strategy extinction, and the *second, third, and fourth rows* (each composed of seven panels) give, respectively, the current strategy richness (r), the current strategy evenness (E_{var}), and the current relative intransitivity (RI) for the initial conditions ('start') and in generations 1, 10, 100, 1000, 10000, and 100000, for various combinations of the initial relative intransitivity of the tournament graph (RI) and quenched randomness of the interaction graph (Q). Colors represent the model outcome (see legends to right of rows); in the case of the RI row, white and grey regions represent, respectively, cases where strategy richness is 1 or 2 (i.e., for which RI is undefined).

For $s = 6, 7, 20,$ and 21 , all possible values of initial intransitivity are considered (respectively numbering 9, 15, 331, and 386 evenly spaced values between 0 and 1, inclusive). For $s = 100$ and 101 , there are too many possible values of initial intransitivity to consider (41651 and 42926, respectively); hence, 401 evenly spaced values between 0 and 1, inclusive, are considered instead. In every case, 101 evenly spaced values of Q between 0 and 1, inclusive, are considered. Within each sub-figure the corresponding RI and Q coordinates from every panel represent the outcome of a single model run.

Note that in the case of $k = 4, 6,$ and 8 ((g) – (x)), there is a threshold value of Q , beyond which strategy coexistence does not occur. However, in the case of $k = 3$ ((a) – (f)), there is no such threshold, at least for this population size (N).

Fig. A3a

$k = 3$

$s = 6$

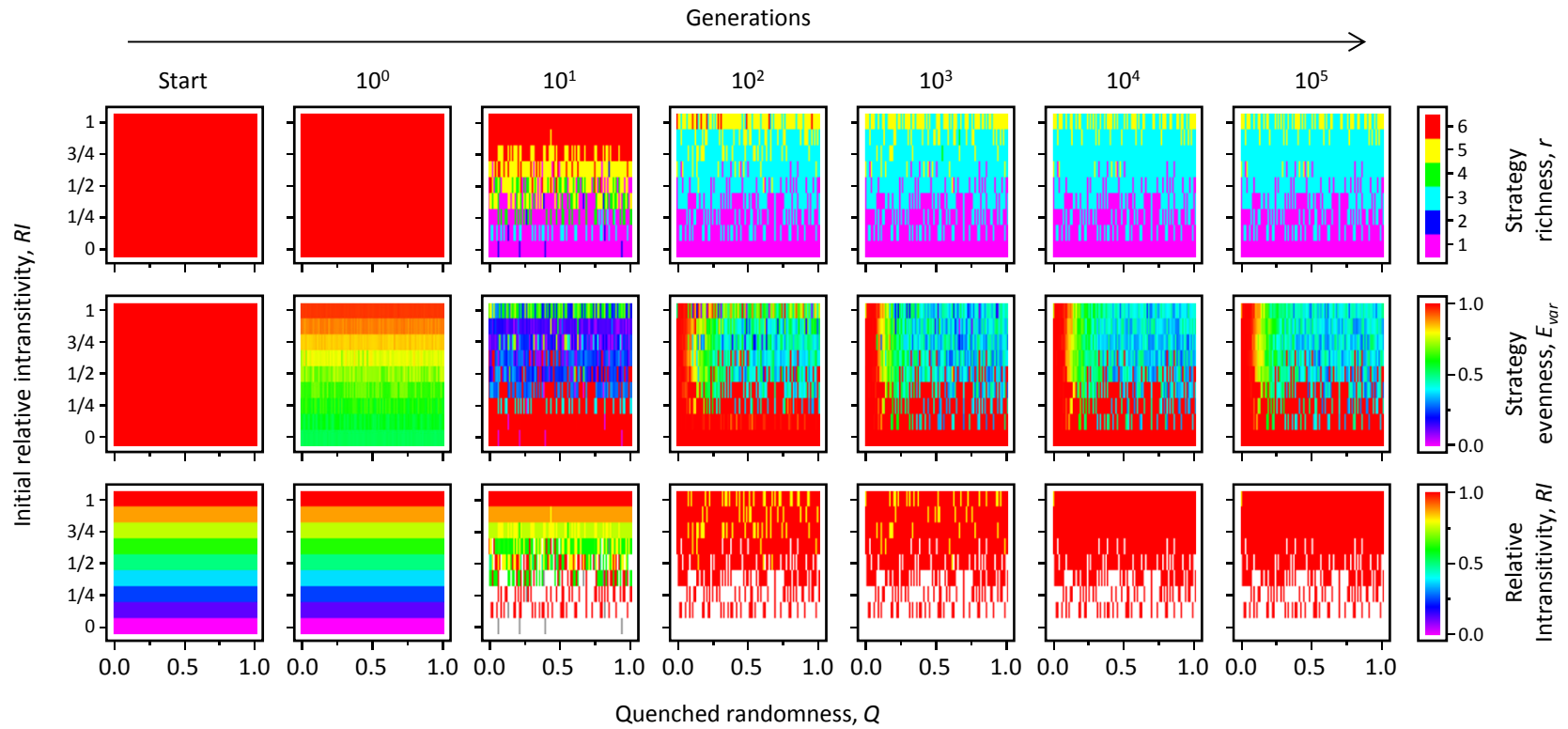
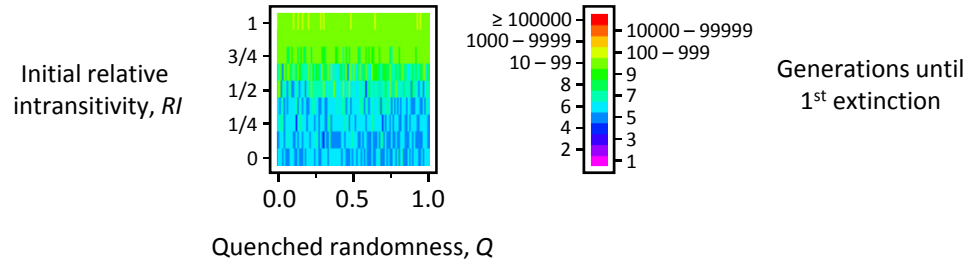


Fig. A3b

$k = 3$

$s = 7$

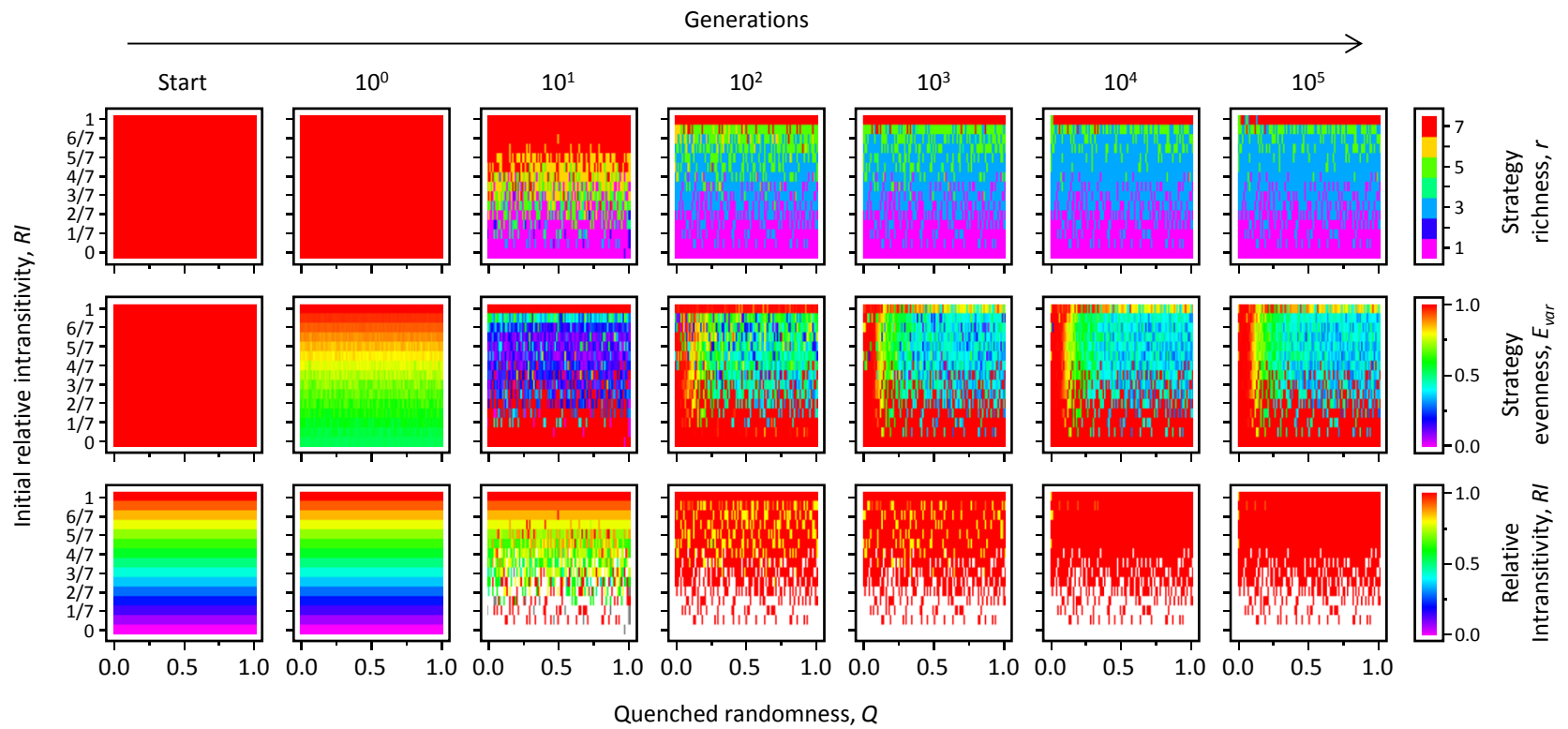
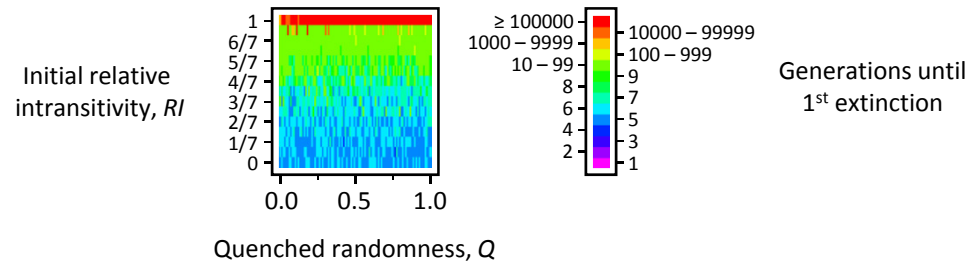


Fig. A3c

$k = 3$
 $s = 20$

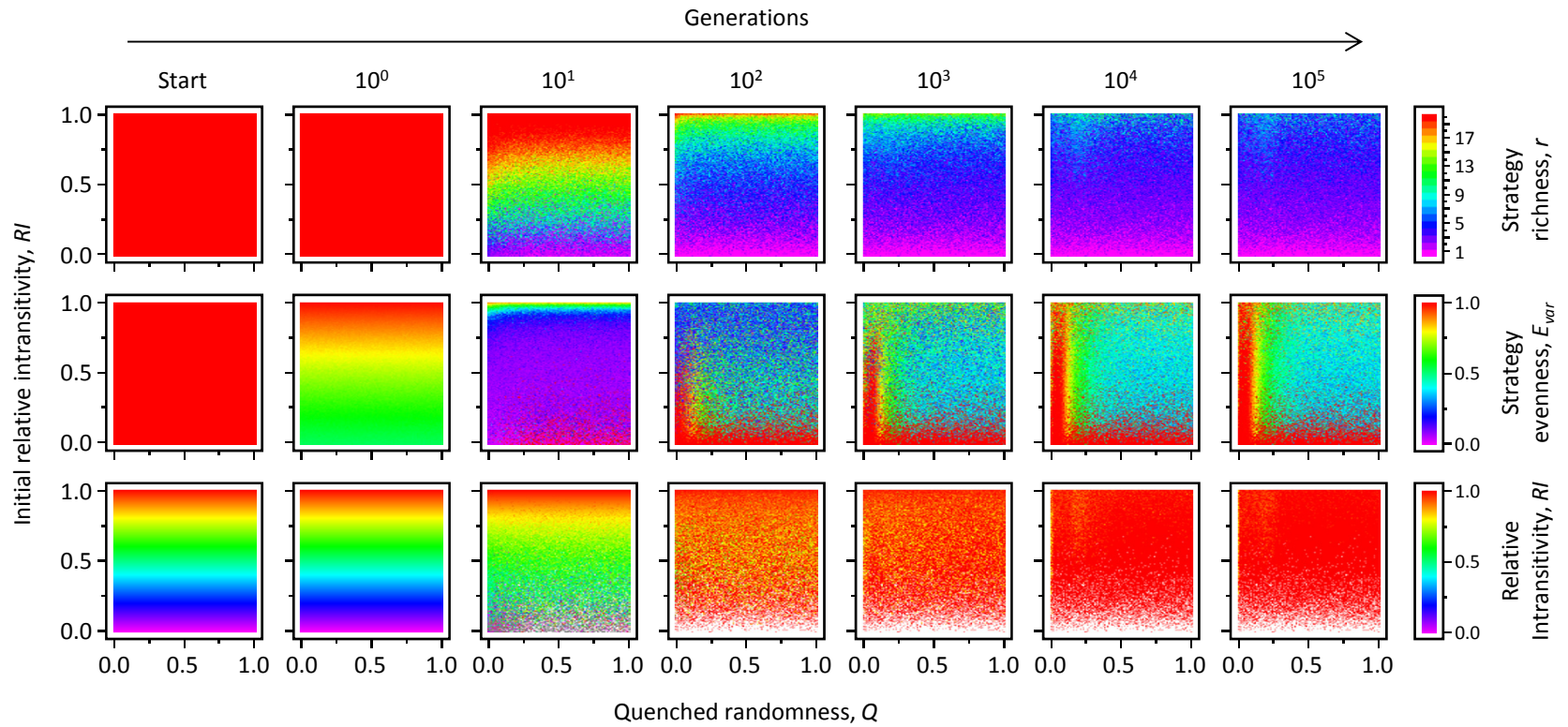
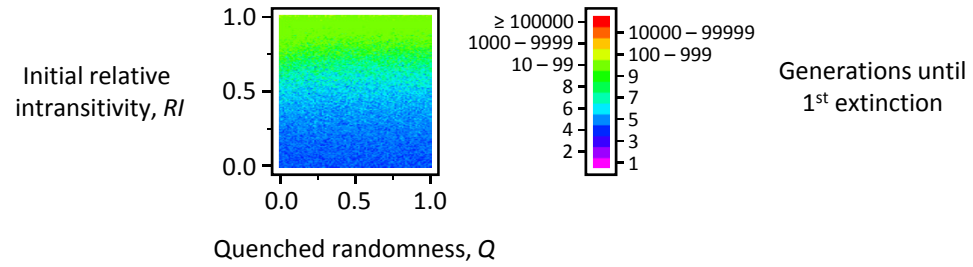


Fig. A3d

$k = 3$
 $s = 21$

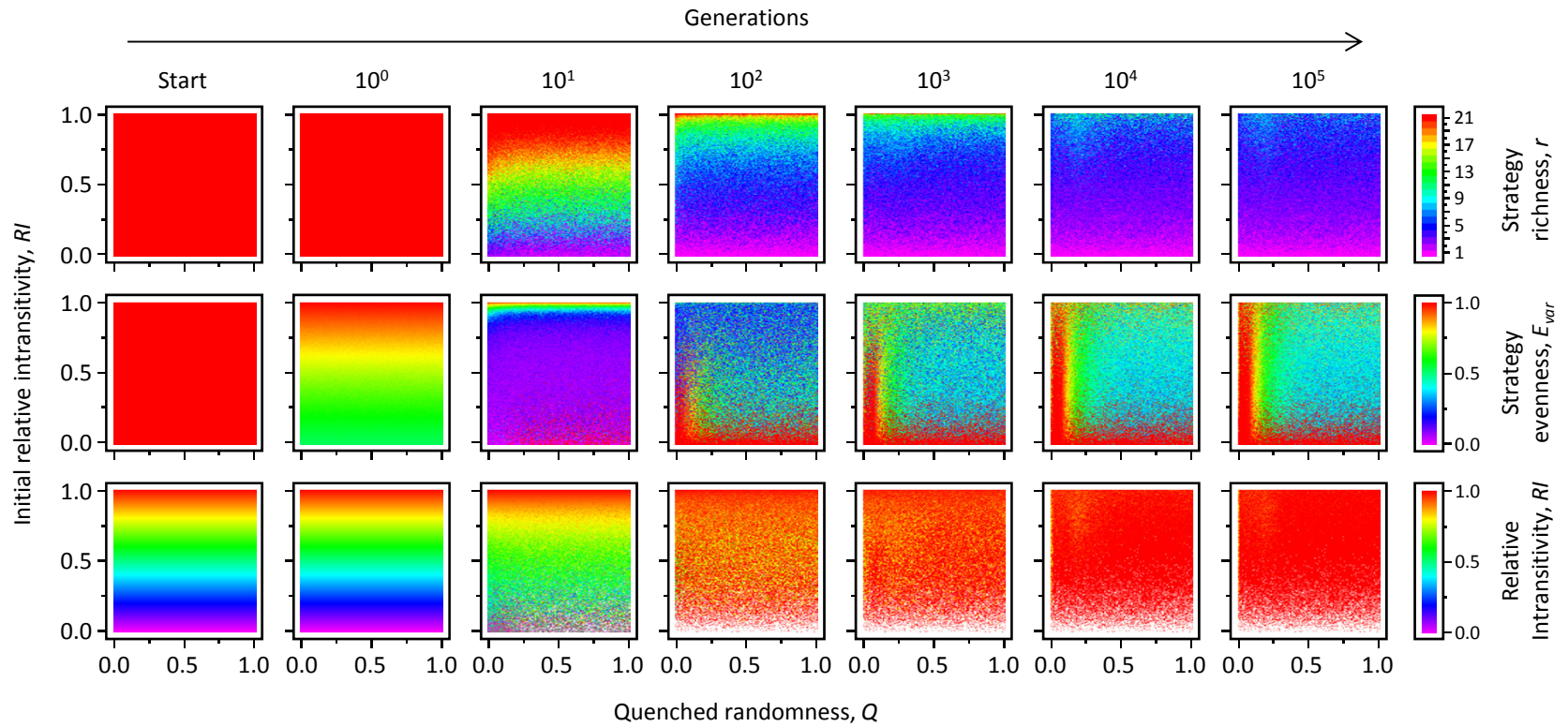
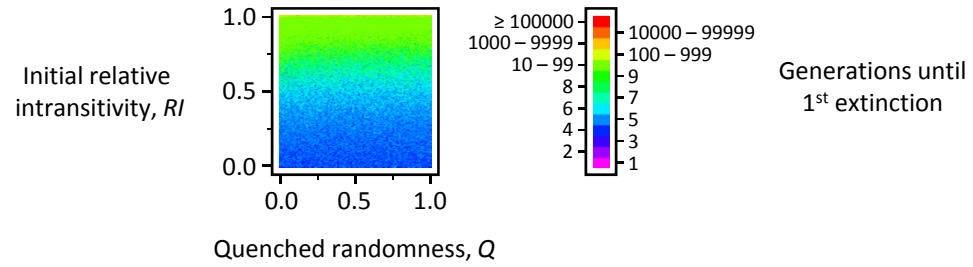


Fig. A3e

$k = 3$
 $s = 100$

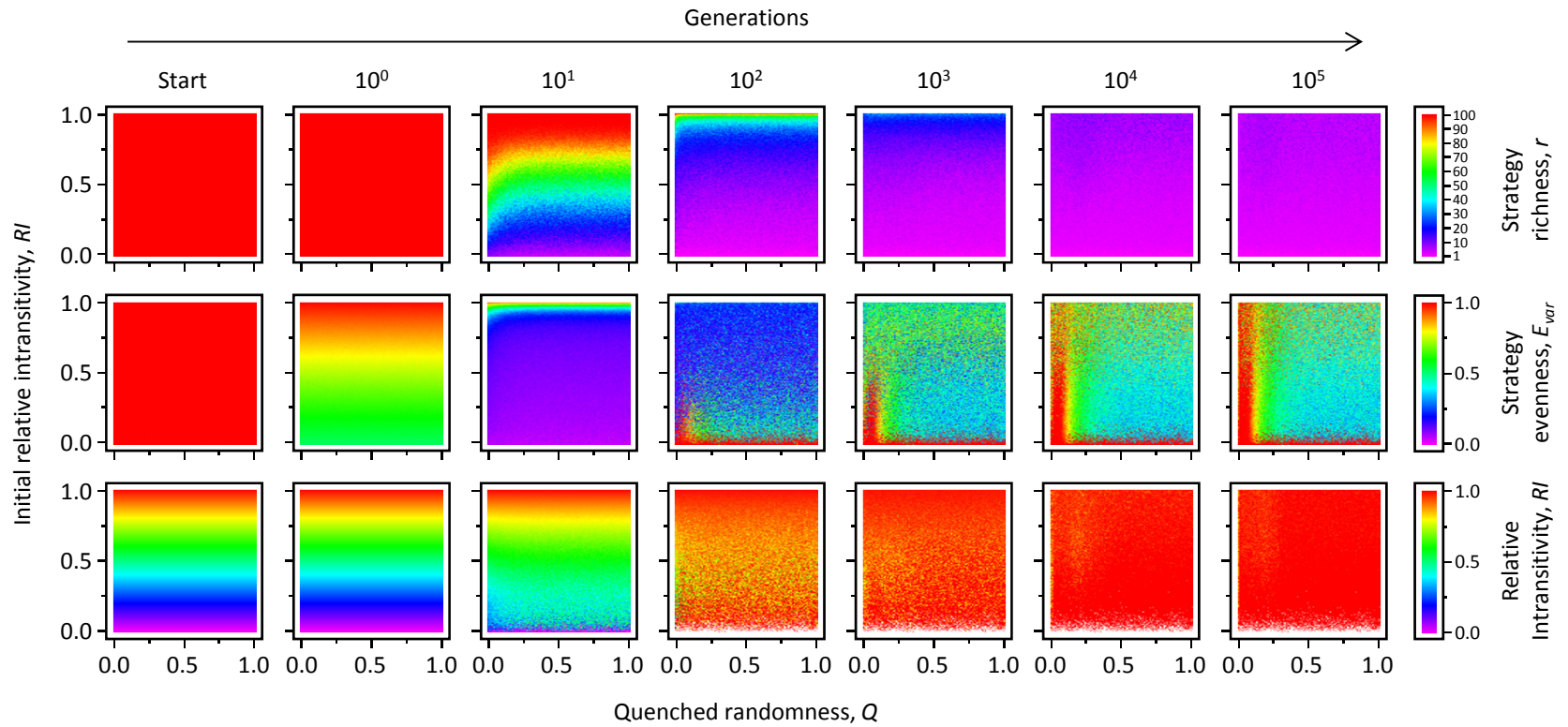
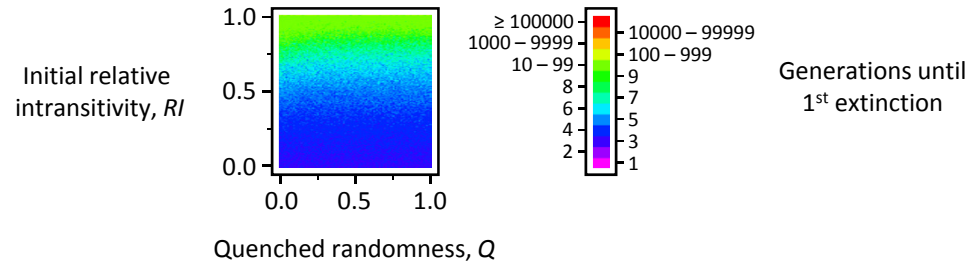


Fig. A3f

$k = 3$
 $s = 101$

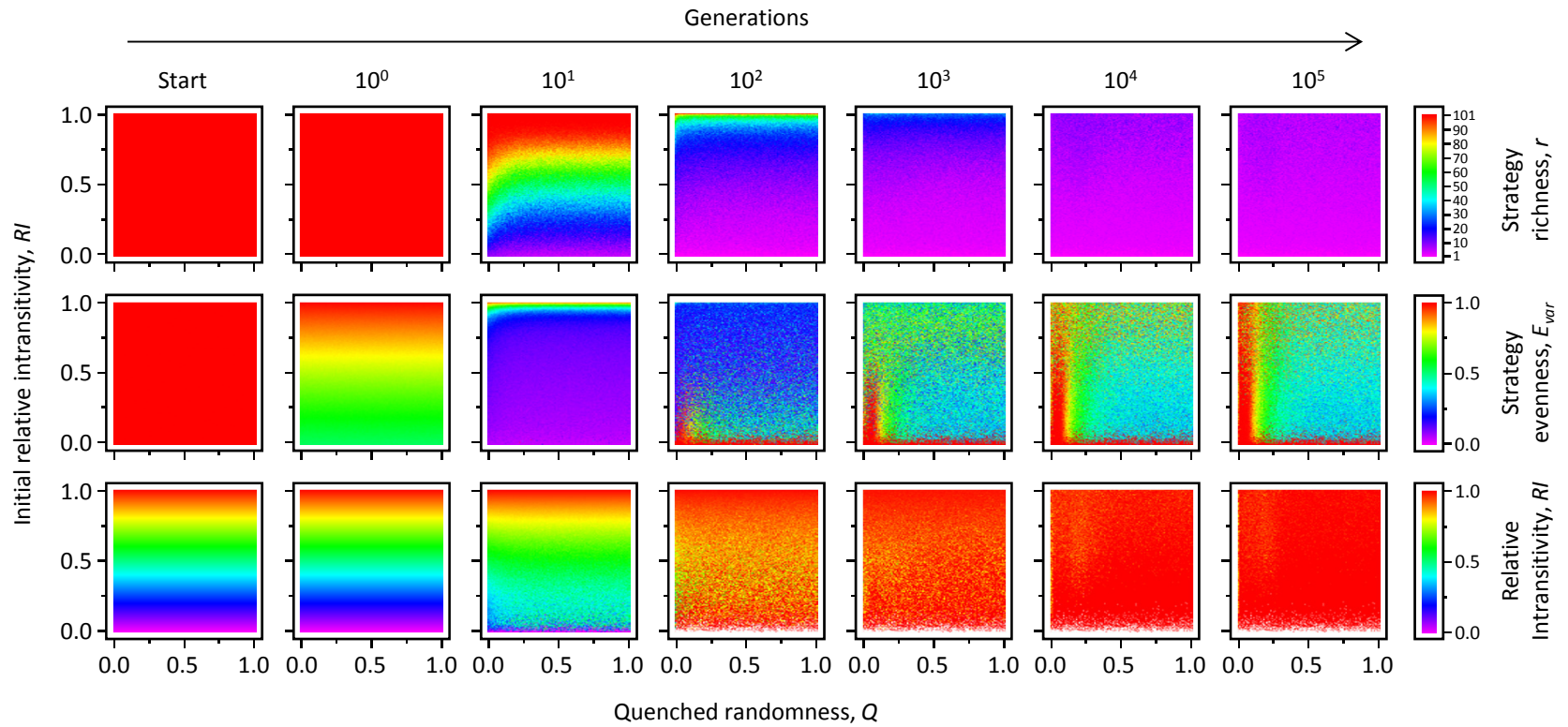
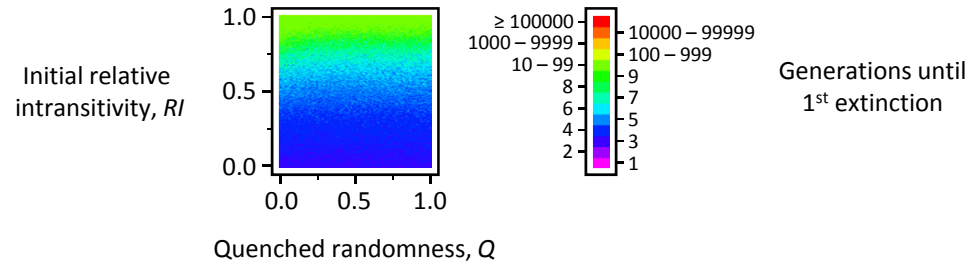


Fig. A3g

$k = 4$

$s = 6$

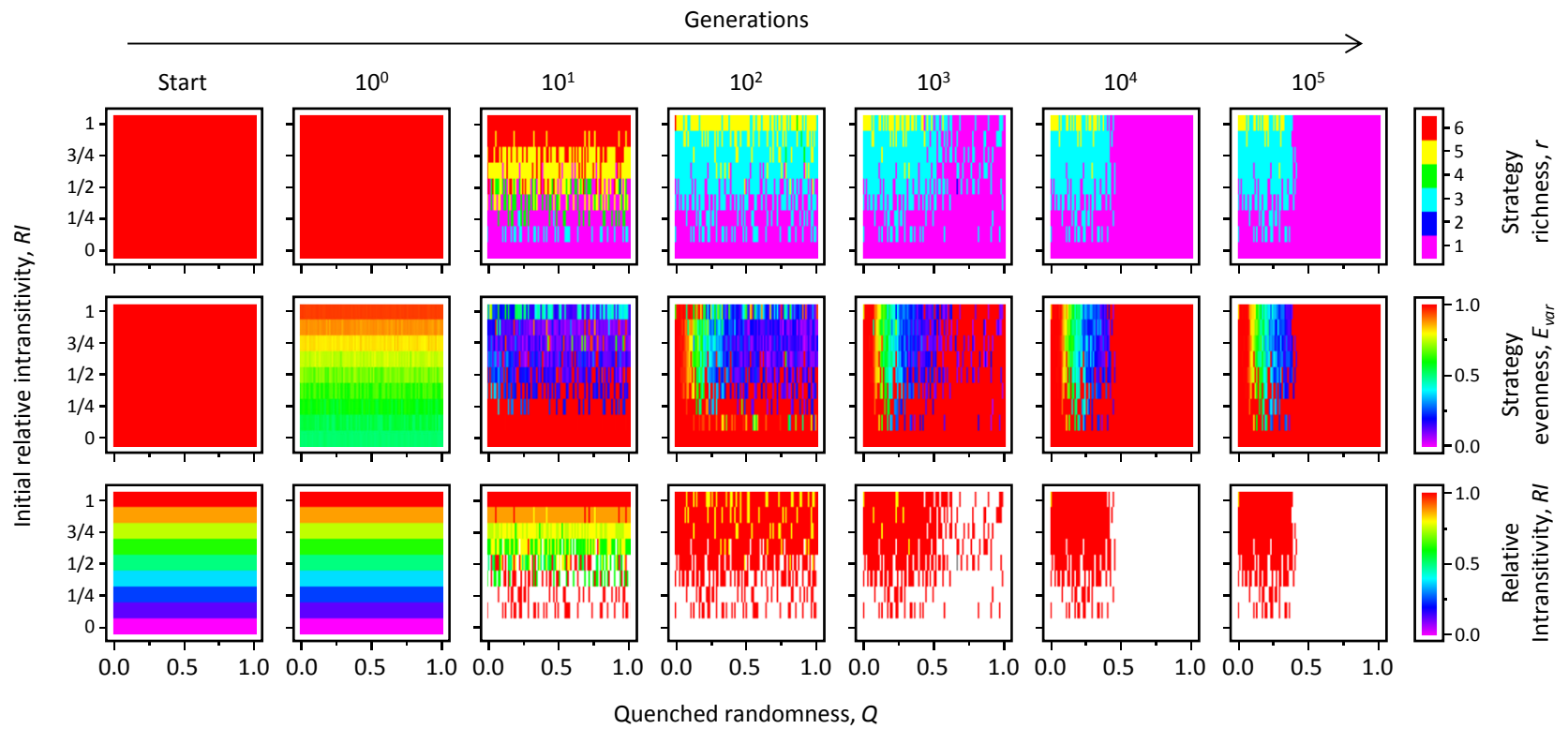
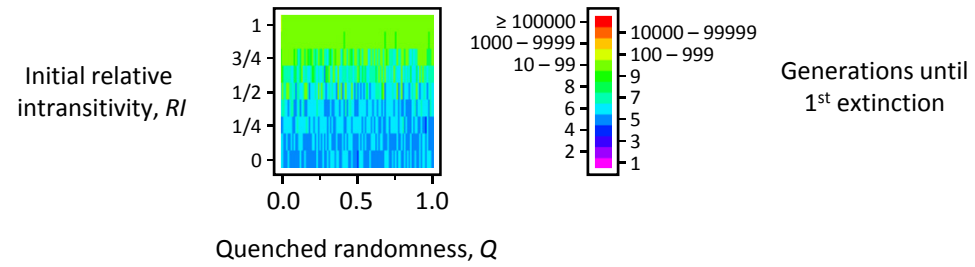


Fig. A3h

$k = 4$

$s = 7$

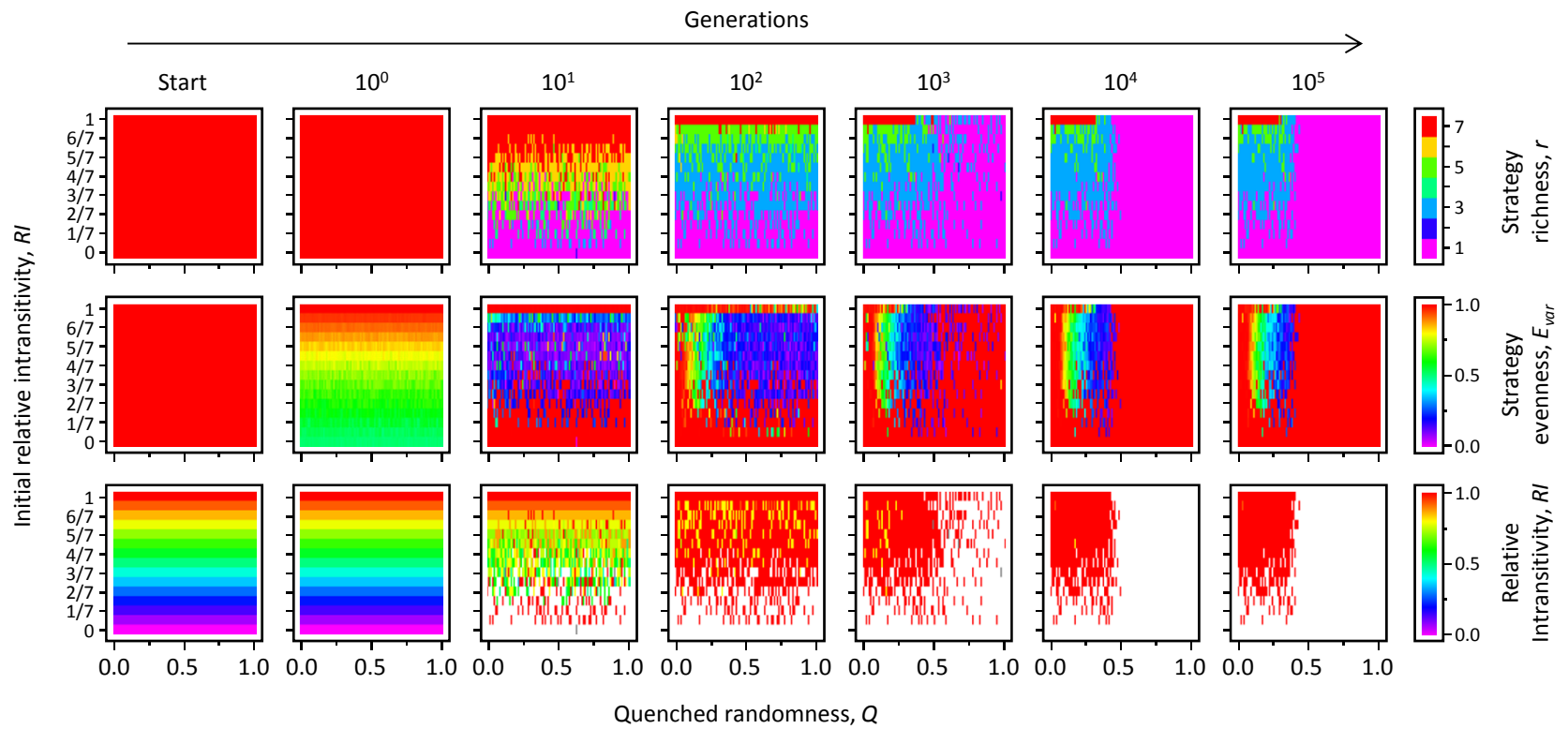
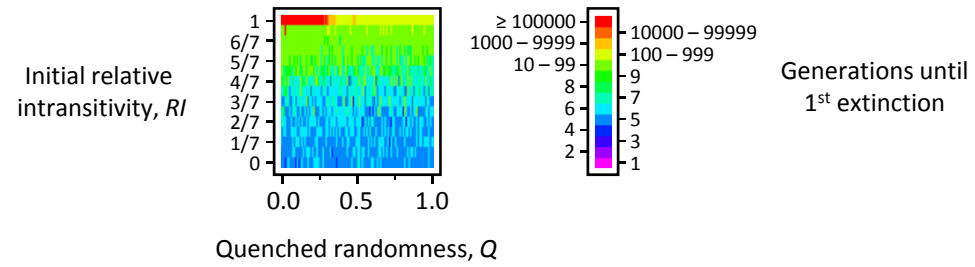


Fig. A3i

$k = 4$
 $s = 20$

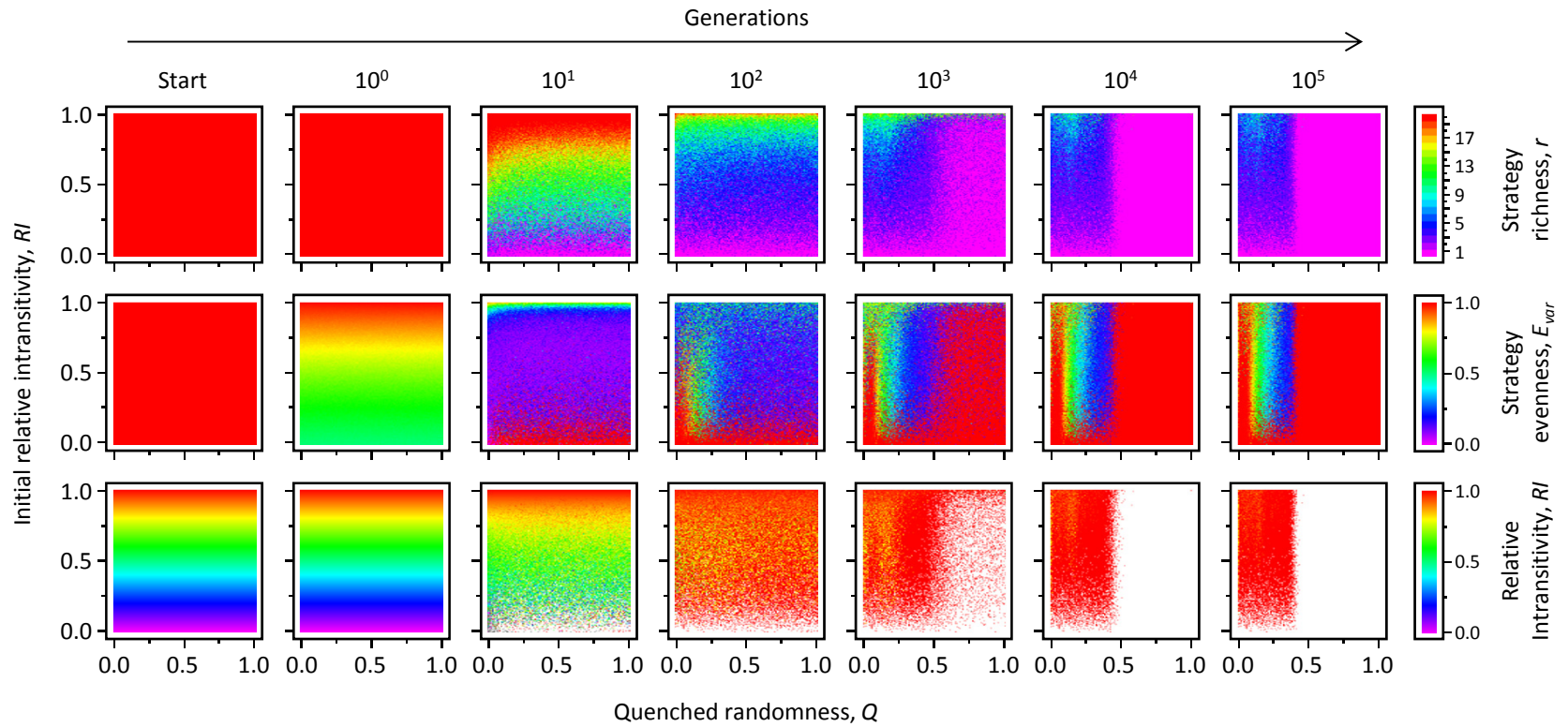
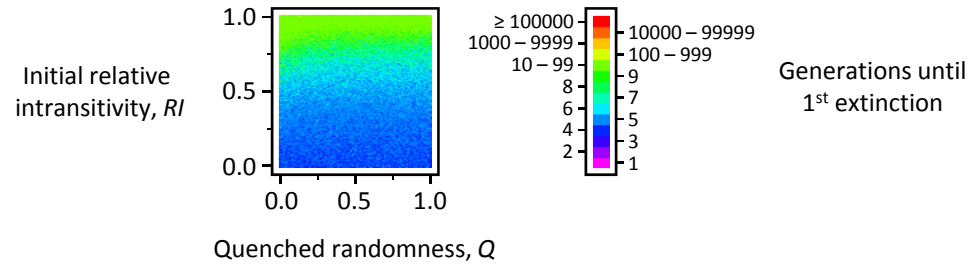


Fig. A3j

$k = 4$
 $s = 21$

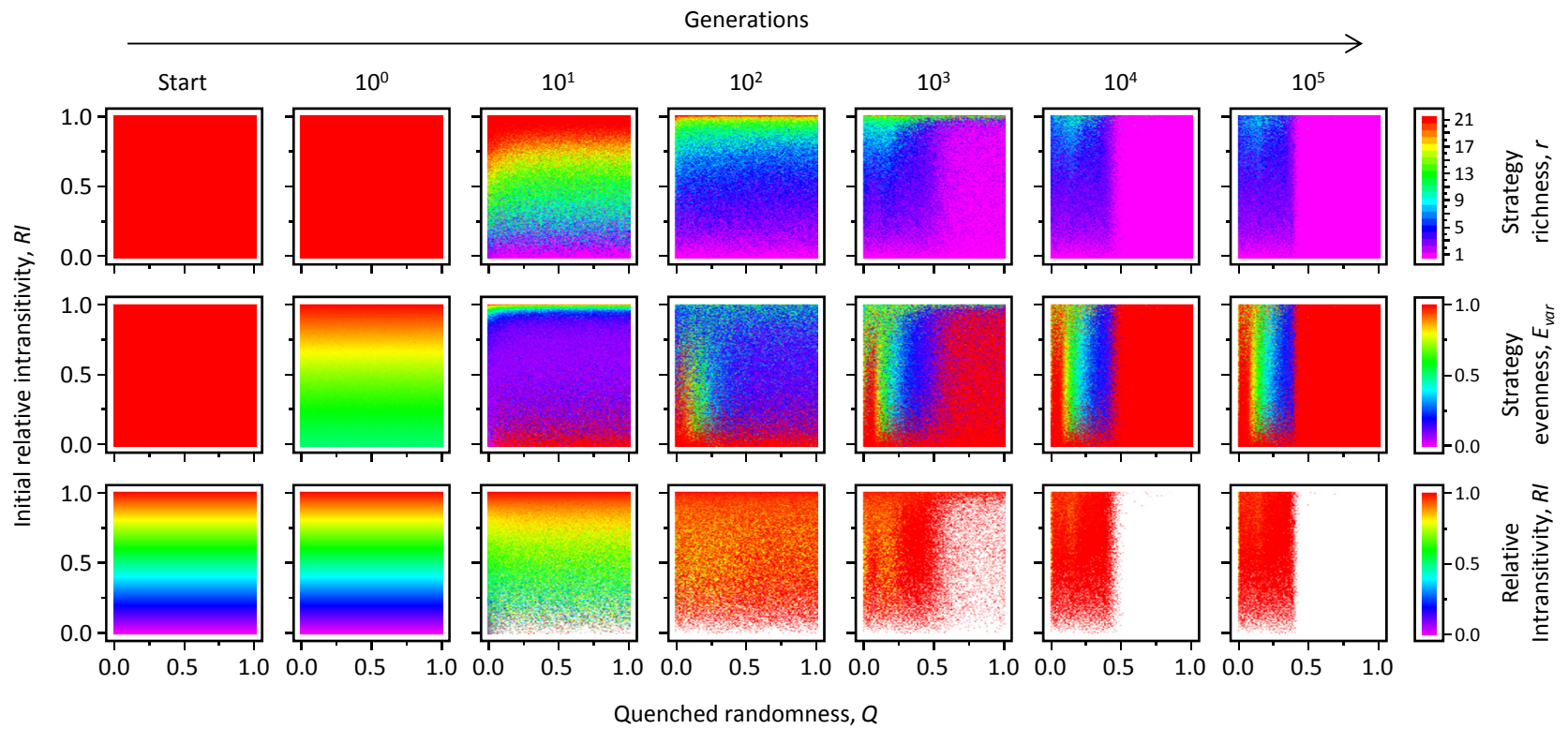
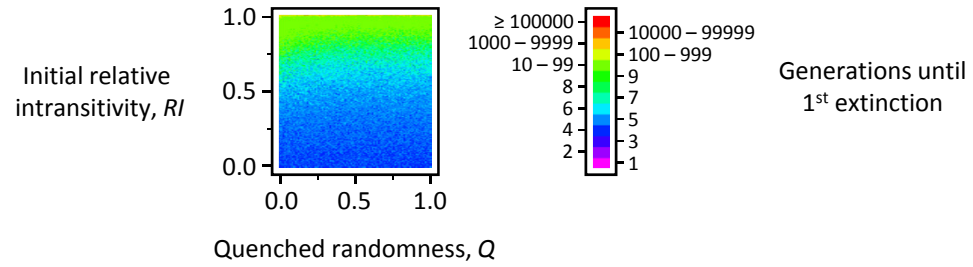


Fig. A3k

$k = 4$
 $s = 100$

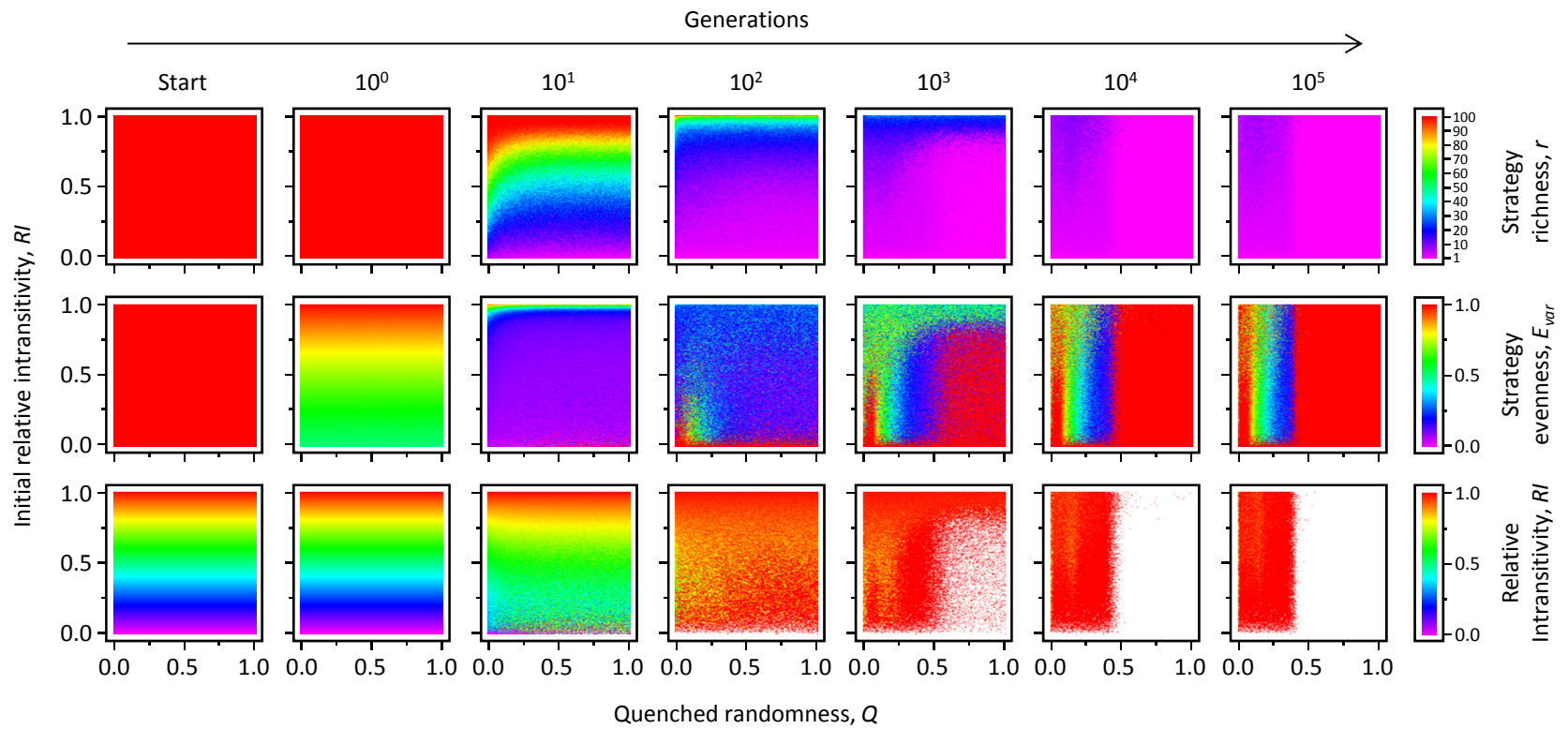
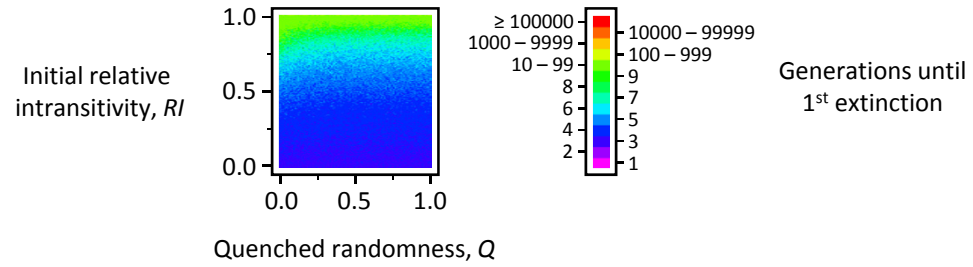


Fig. A3I

$k = 4$
 $s = 101$

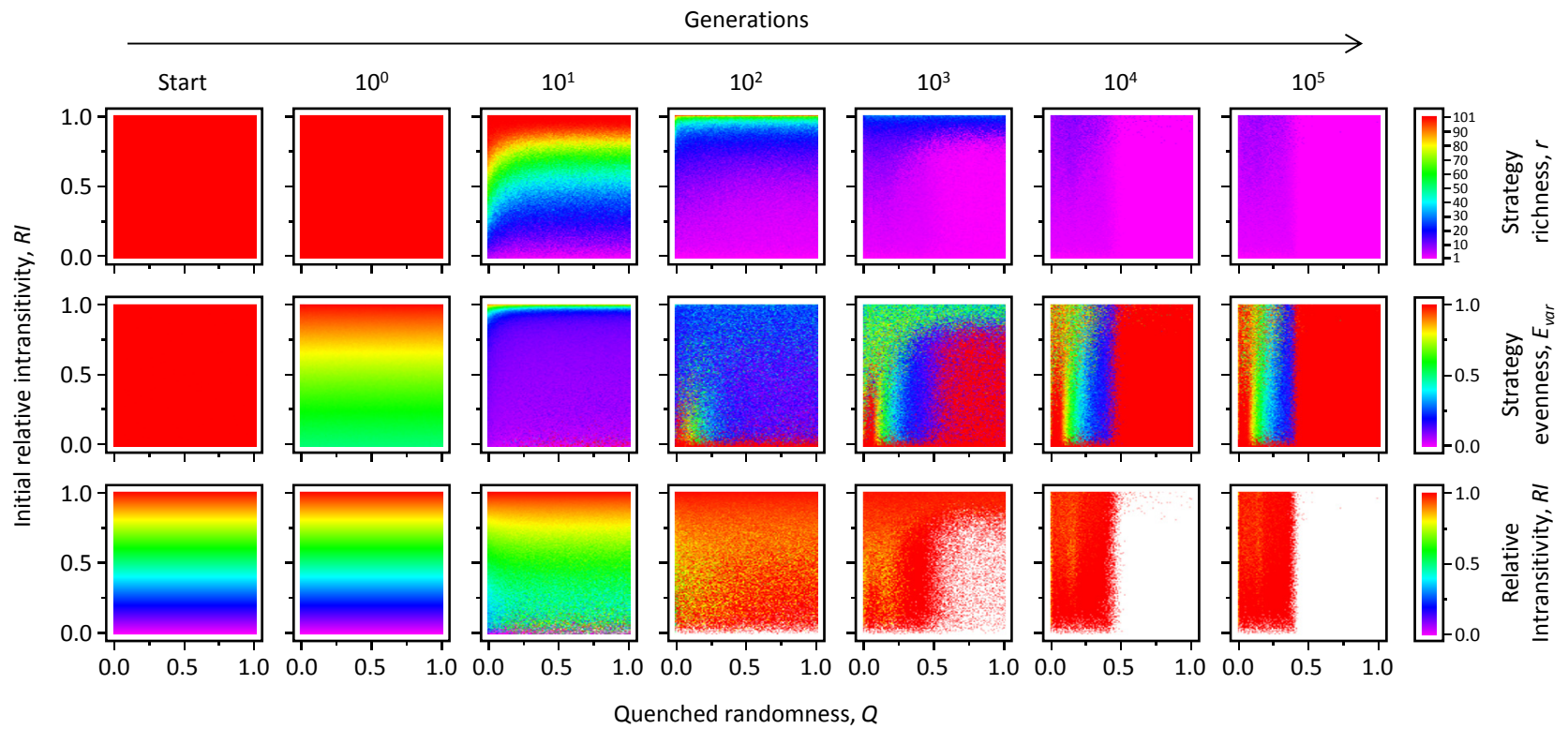
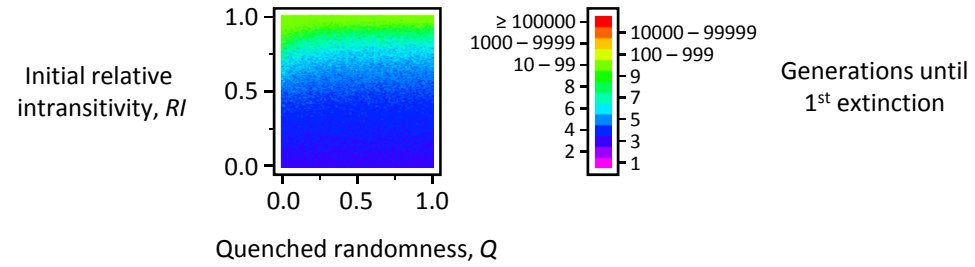


Fig. A3m

$k = 6$

$s = 6$

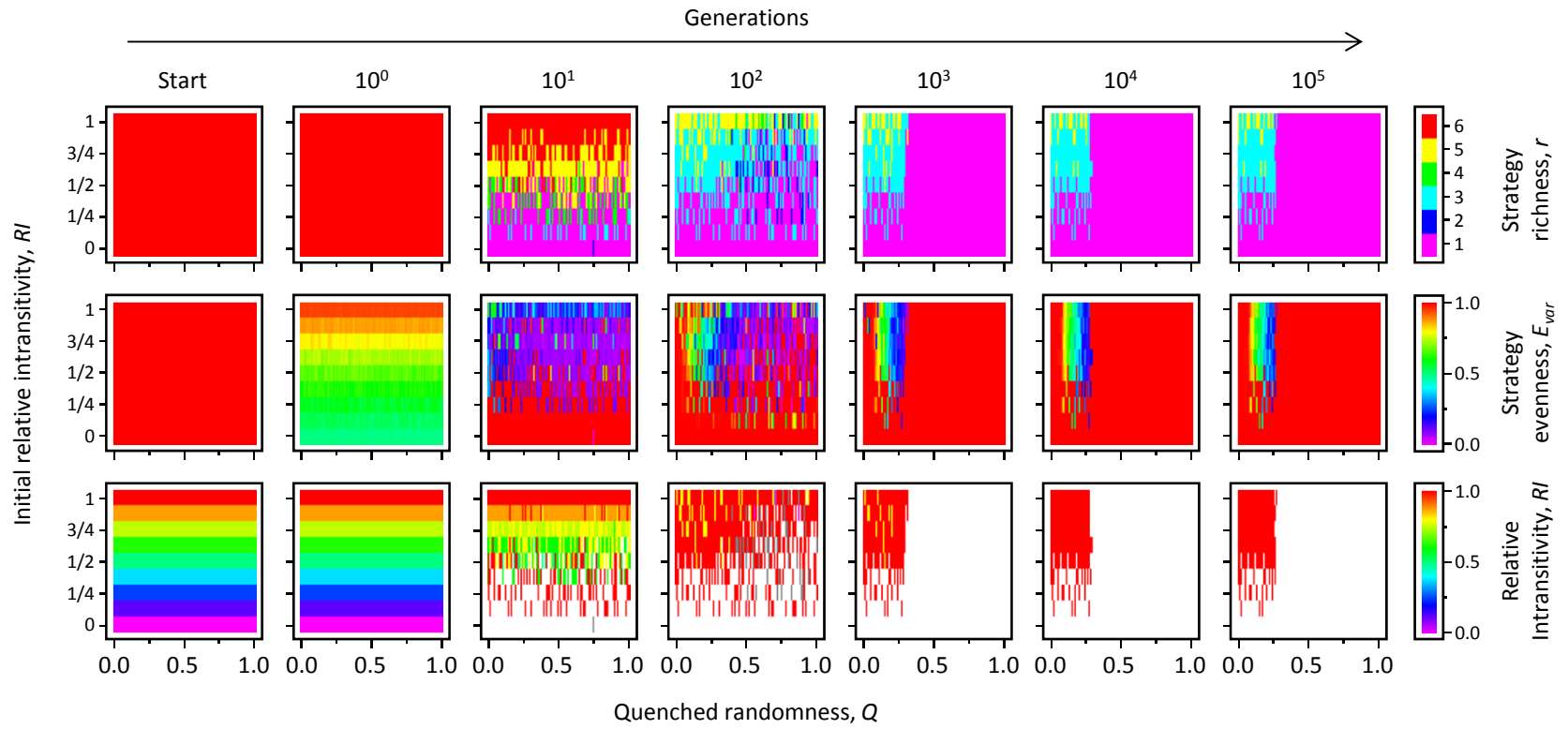
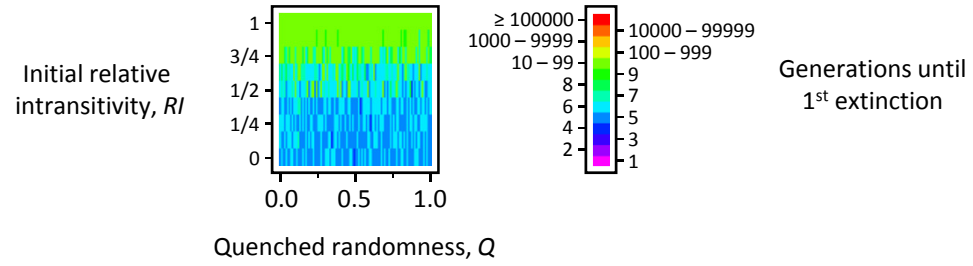


Fig. A3n

$k = 6$
 $s = 7$

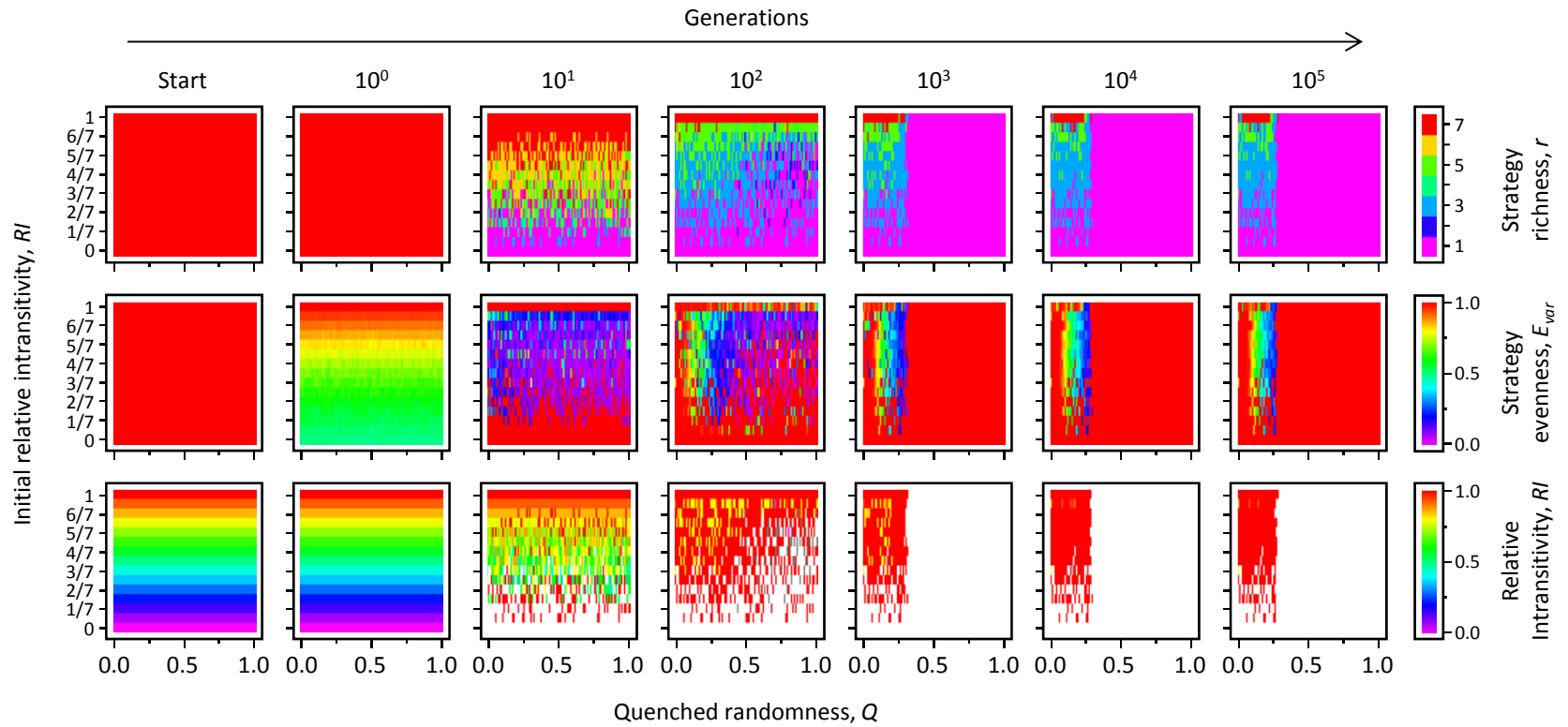
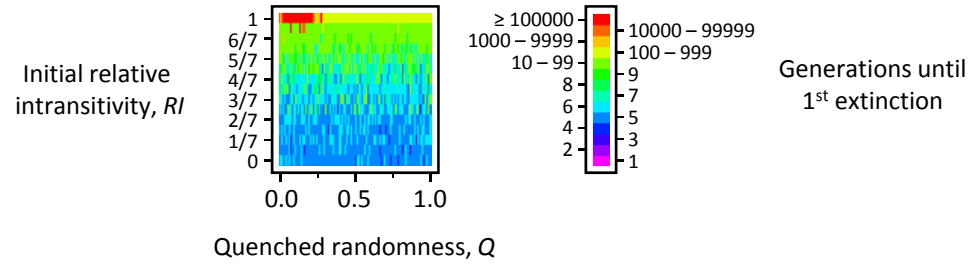


Fig. A3o

$k = 6$
 $s = 20$

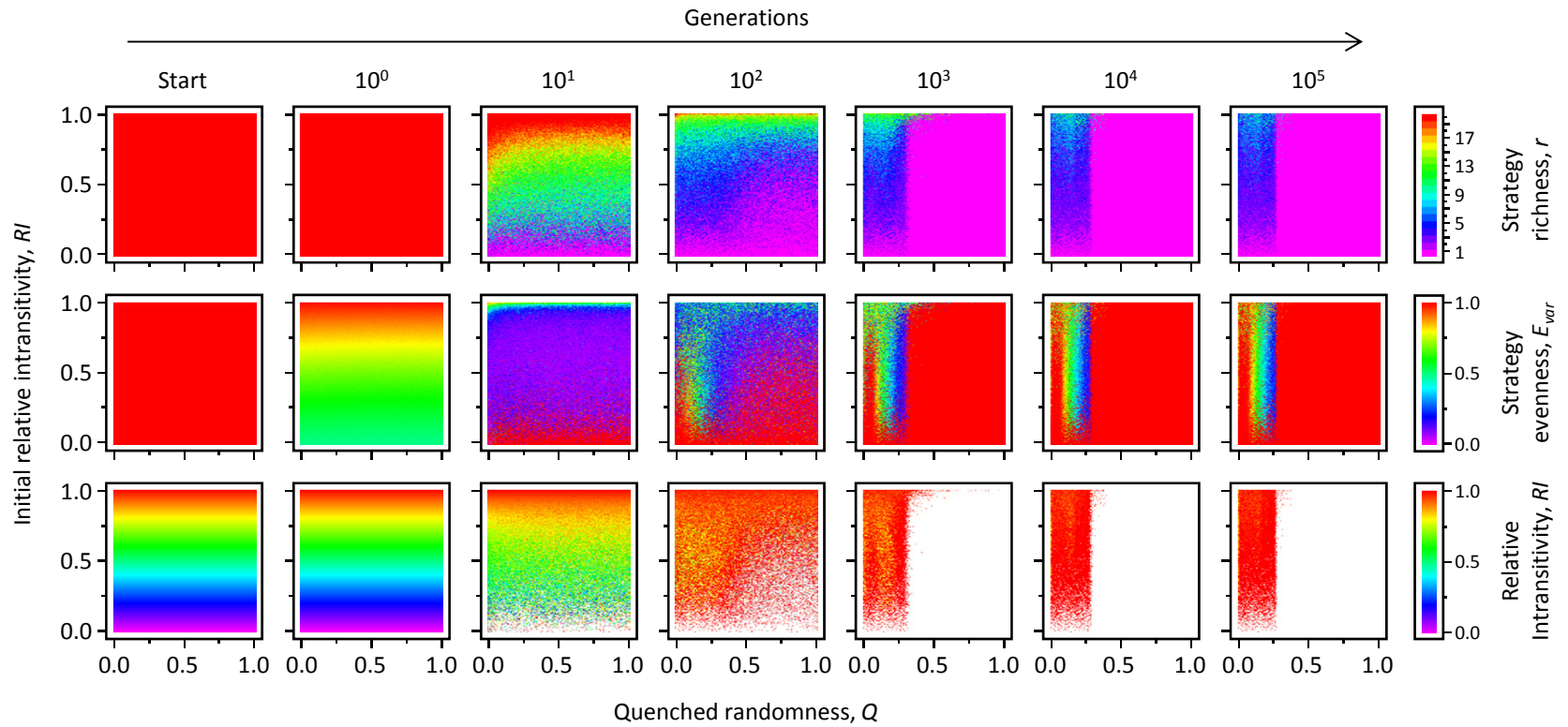
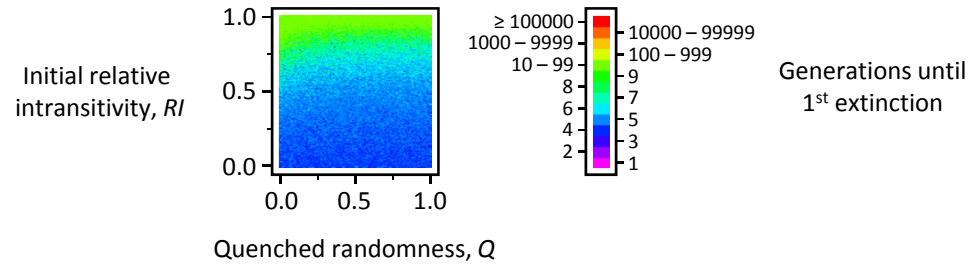


Fig. A3p

$k = 6$
 $s = 21$

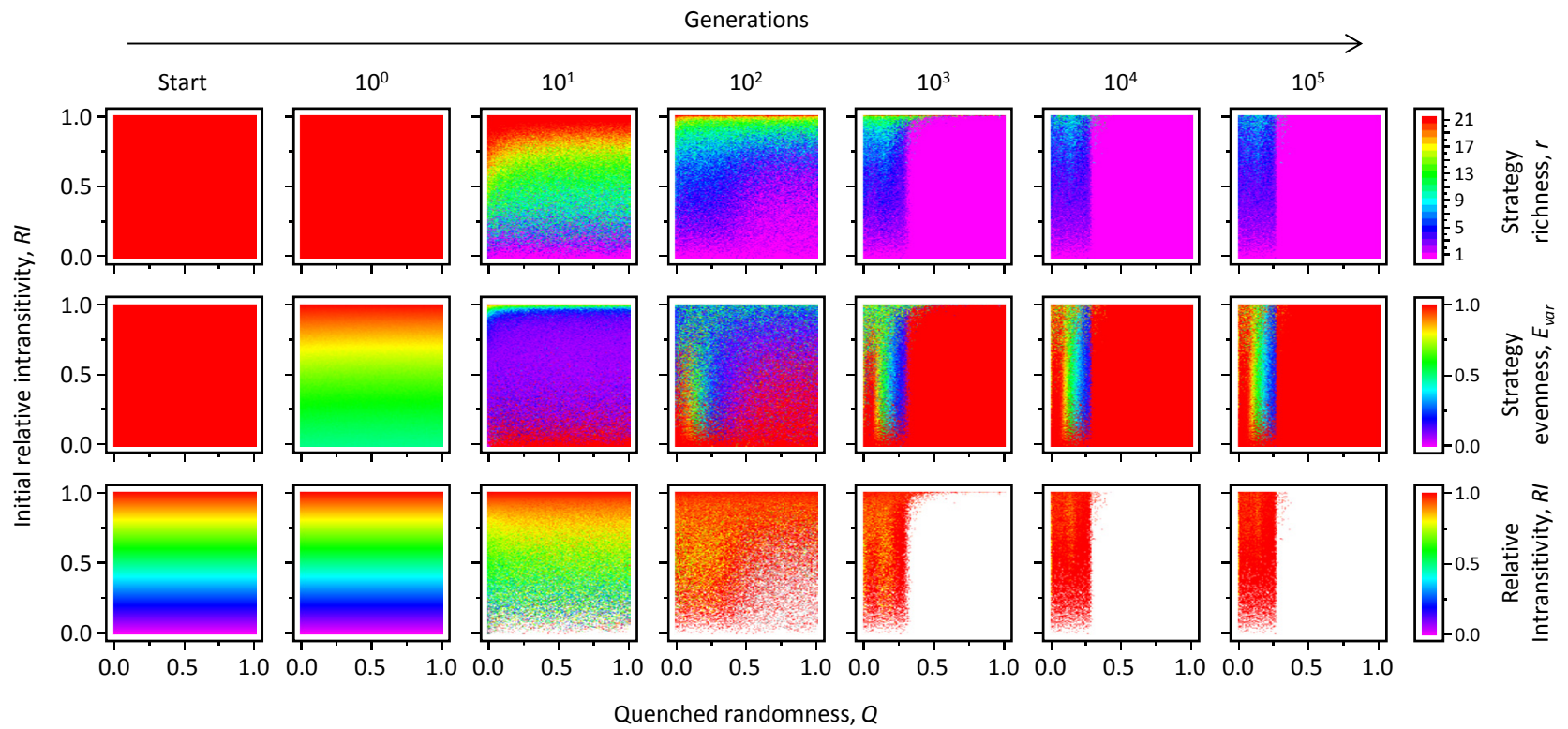
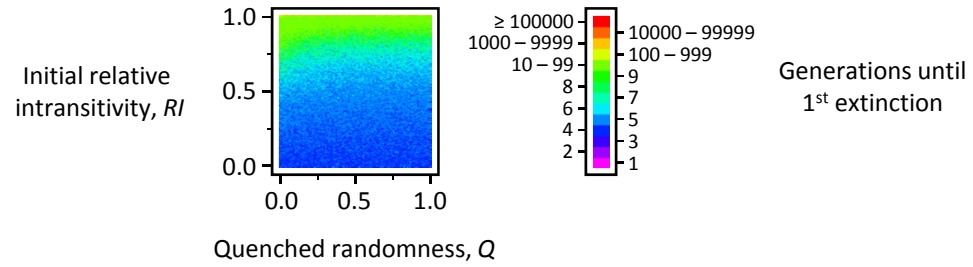


Fig. A3q

$k = 6$
 $s = 100$

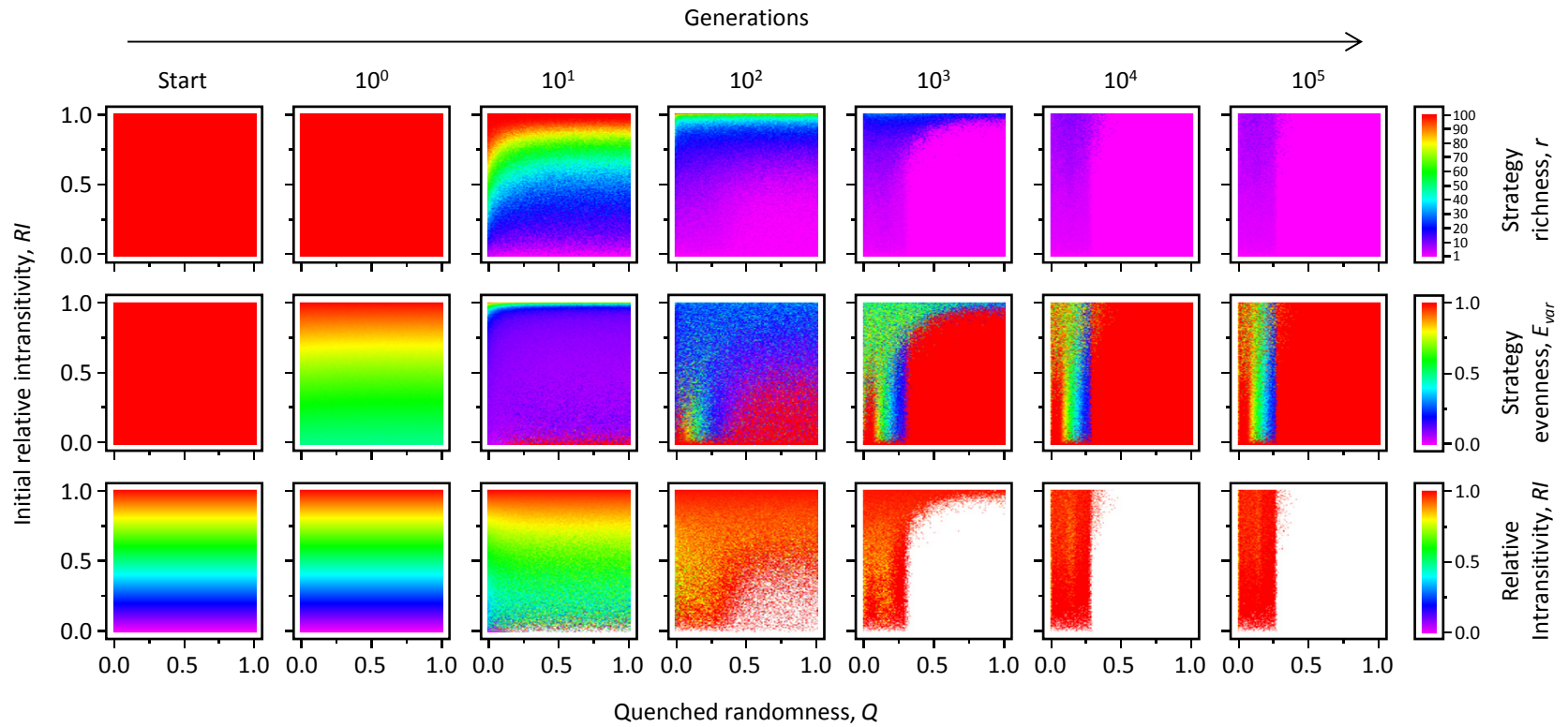
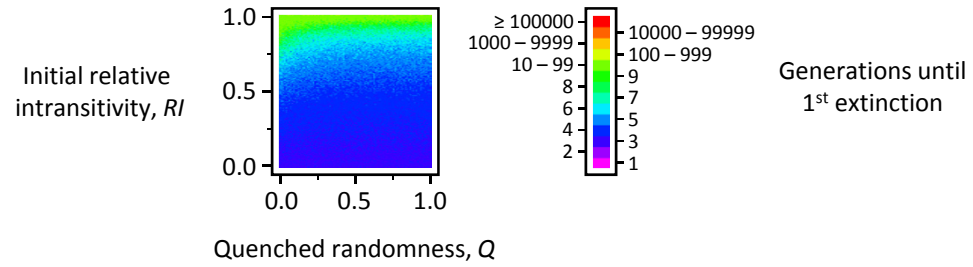


Fig. A3r

$k = 6$
 $s = 101$

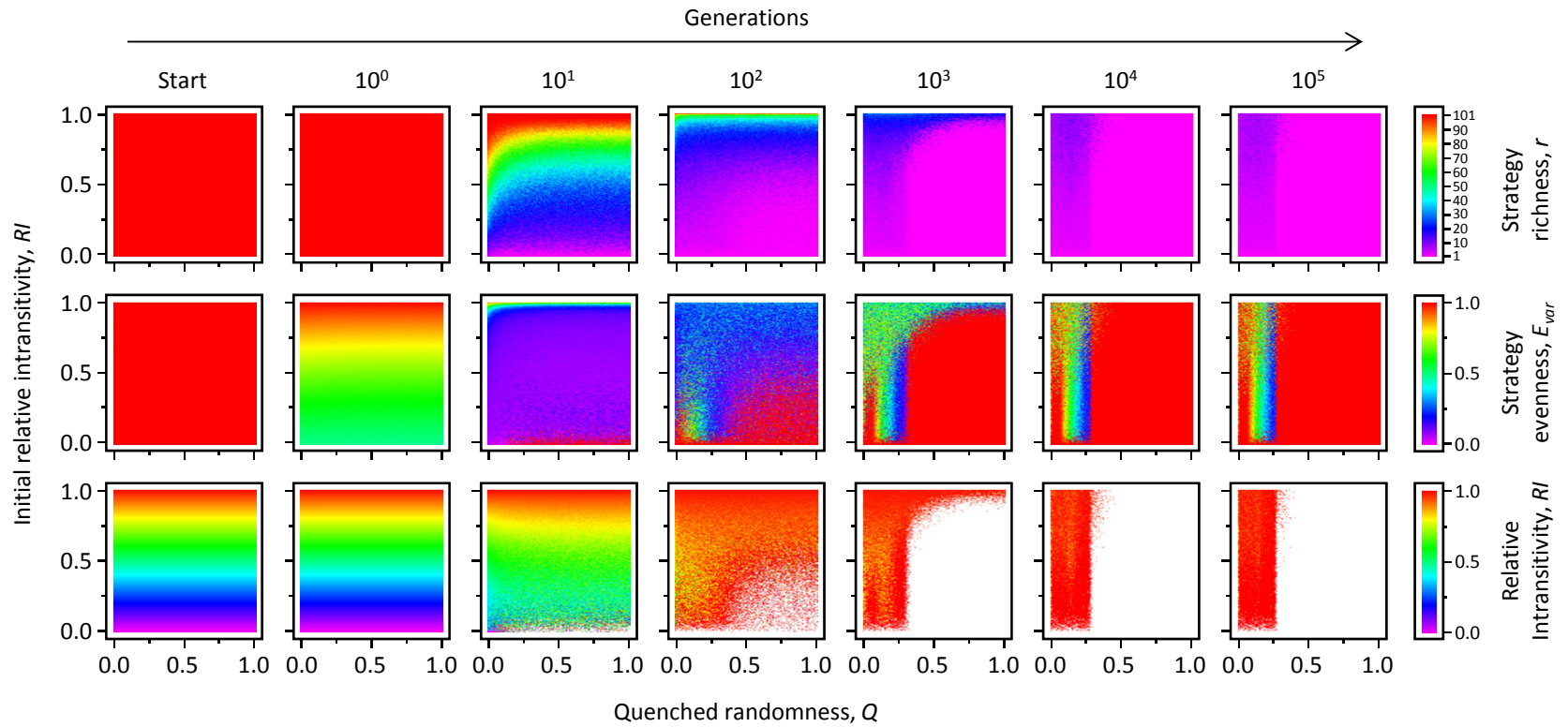
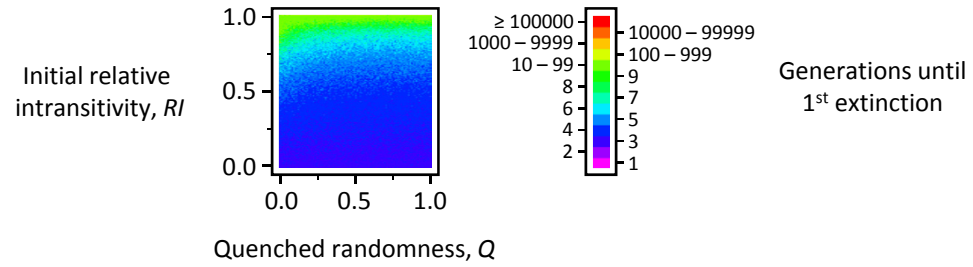


Fig. A3s

$k = 8$

$s = 6$

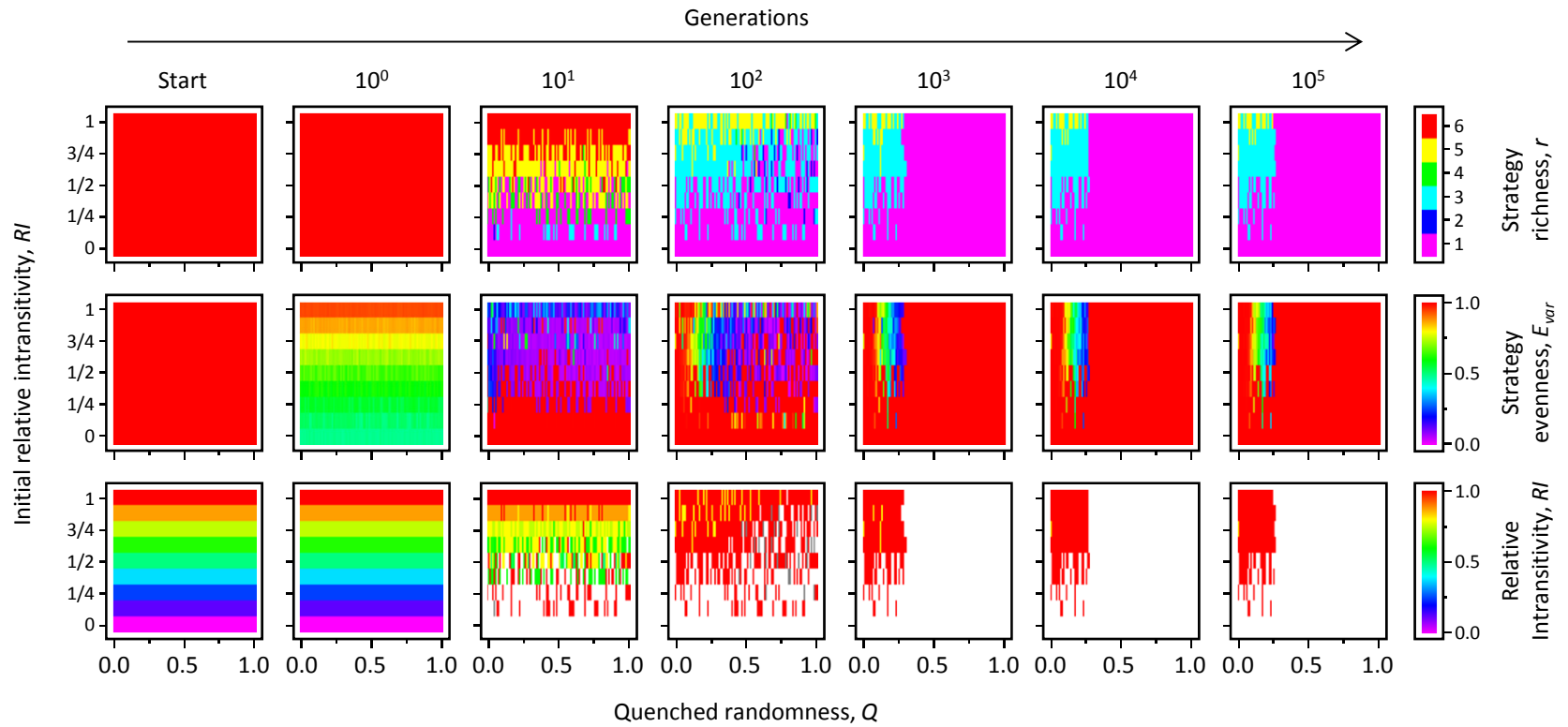
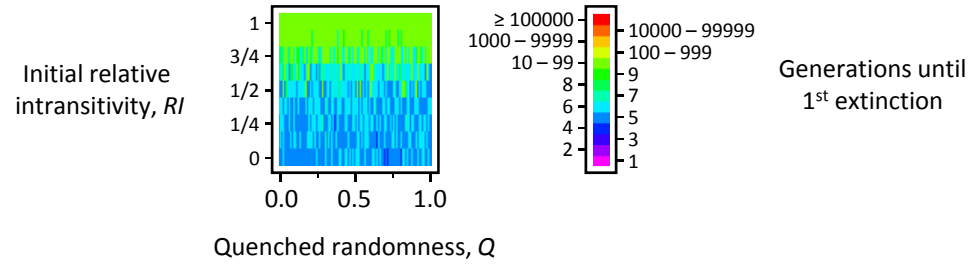


Fig. A3t

$k = 8$

$s = 7$

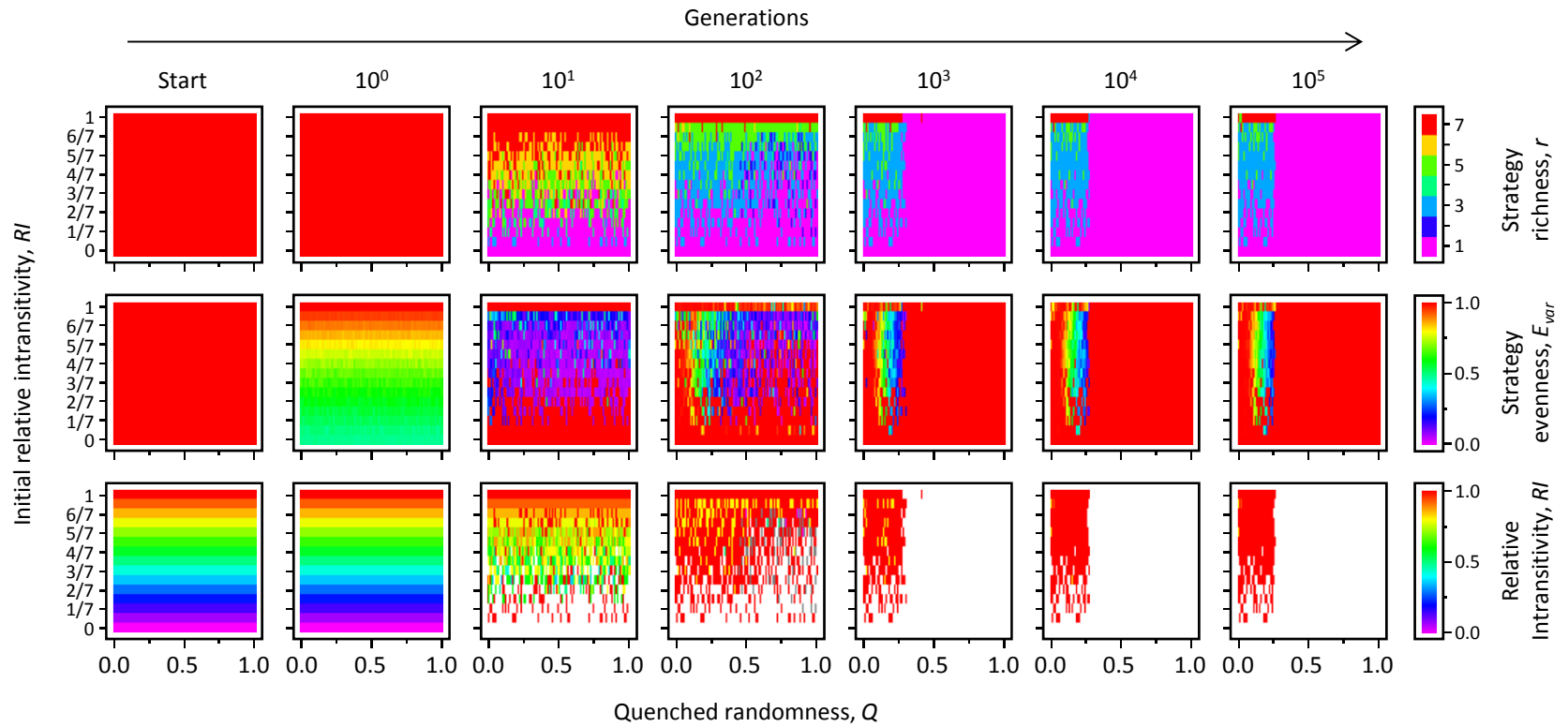
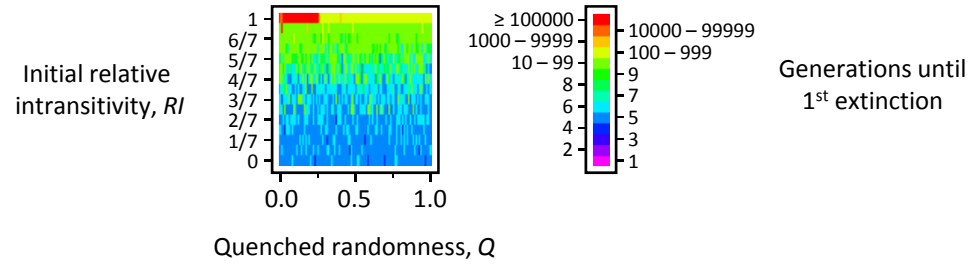


Fig. A3u

$k = 8$
 $s = 20$

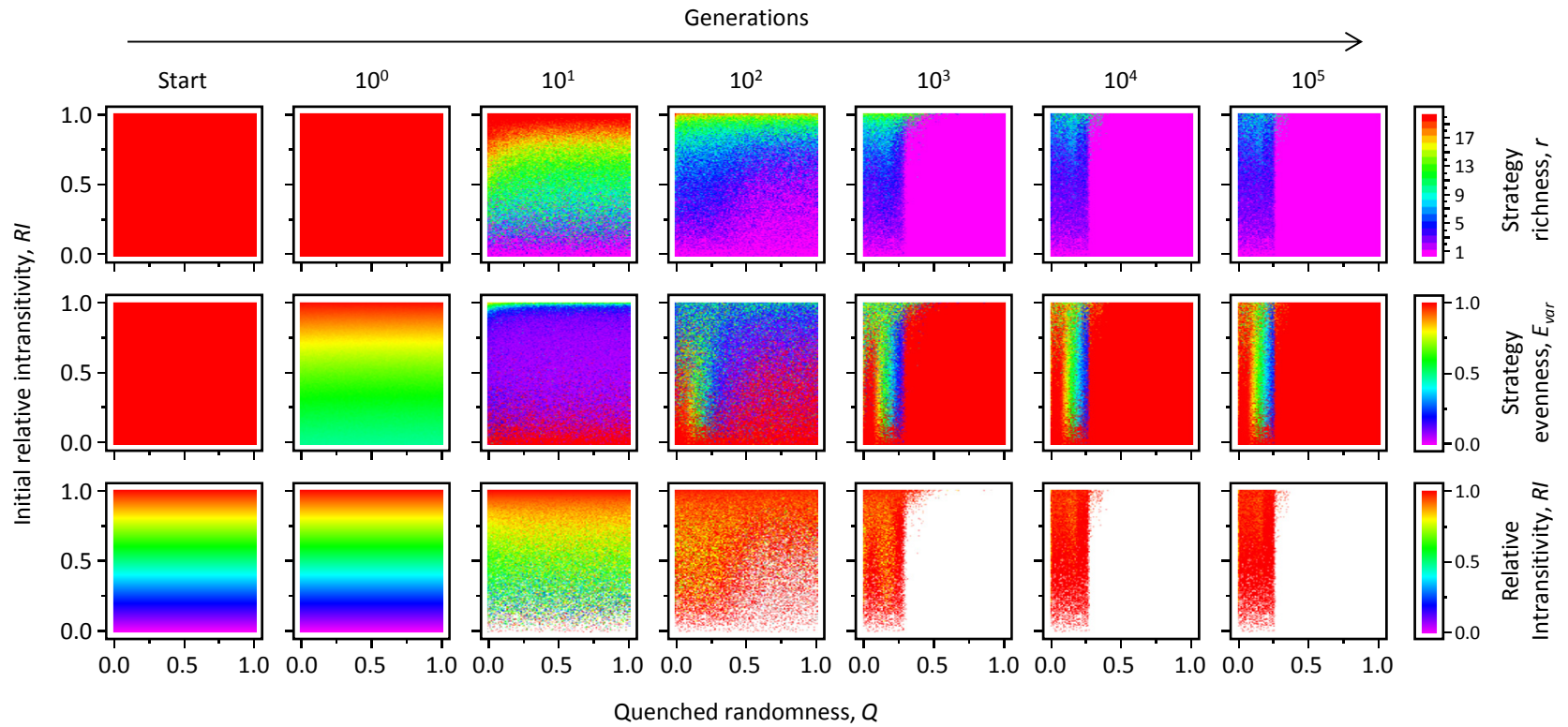
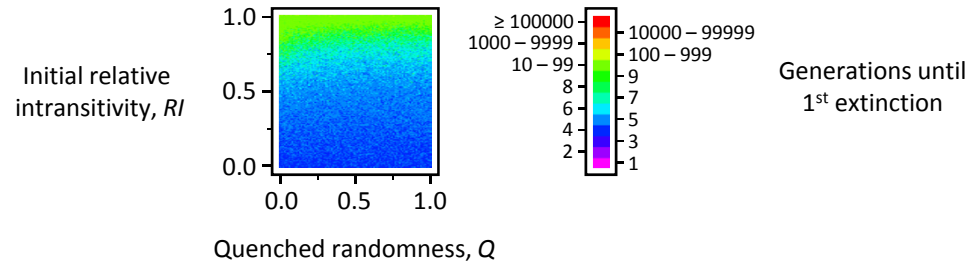


Fig. A3v

$k = 8$
 $s = 21$

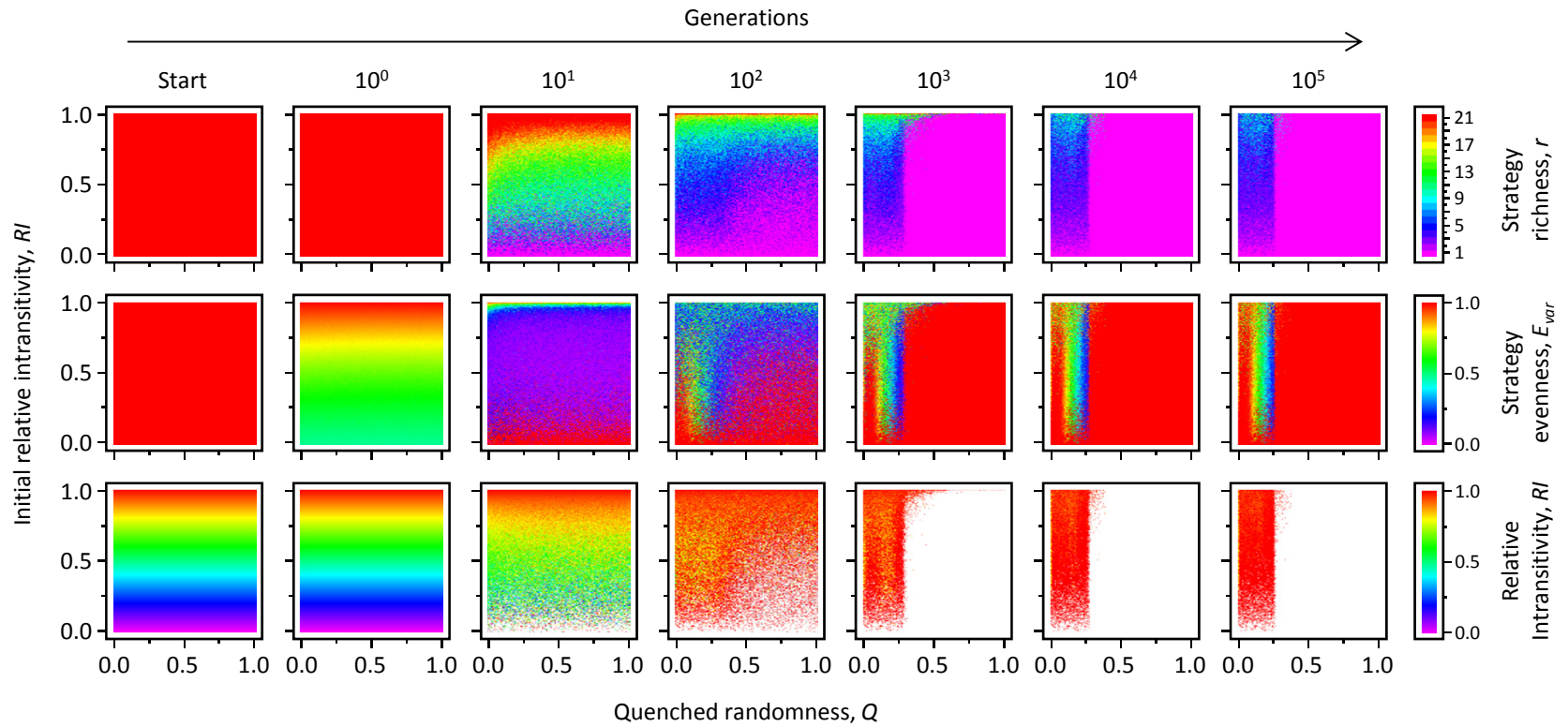
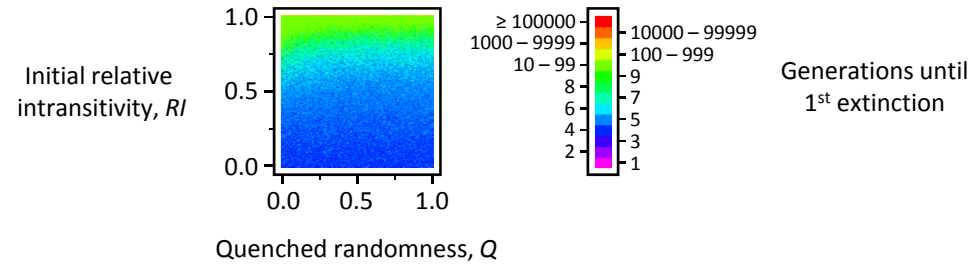


Fig. A3w

$k = 8$
 $s = 100$

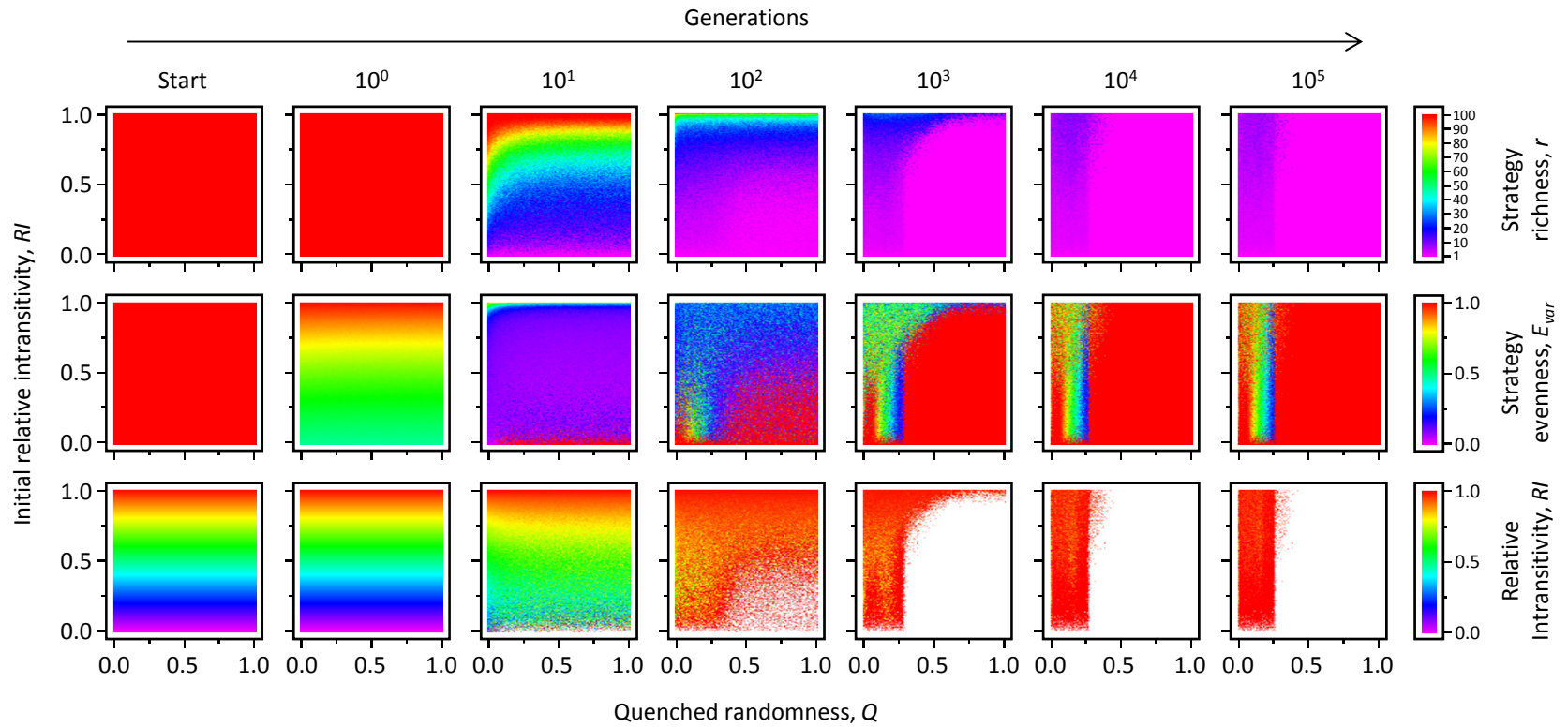
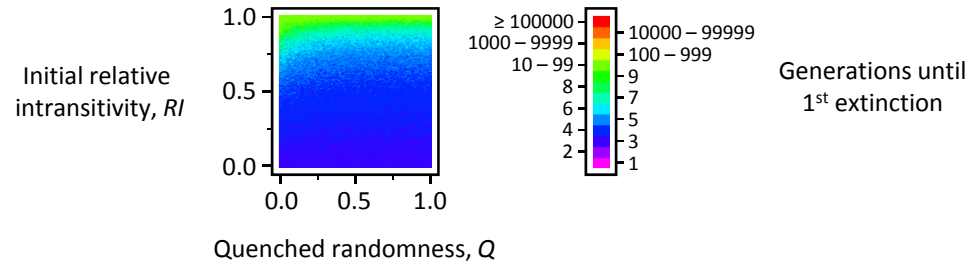


Fig. A3x

$k = 8$
 $s = 101$

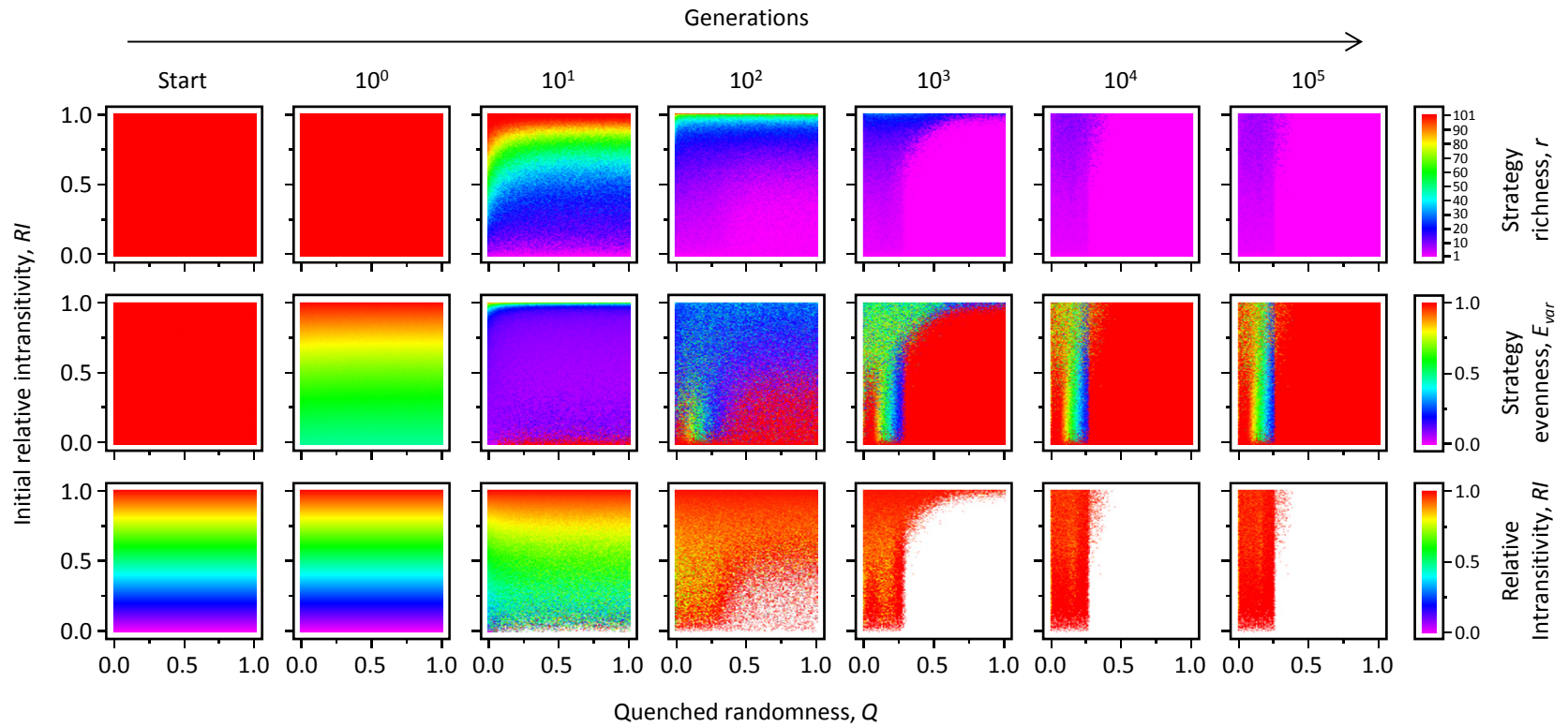
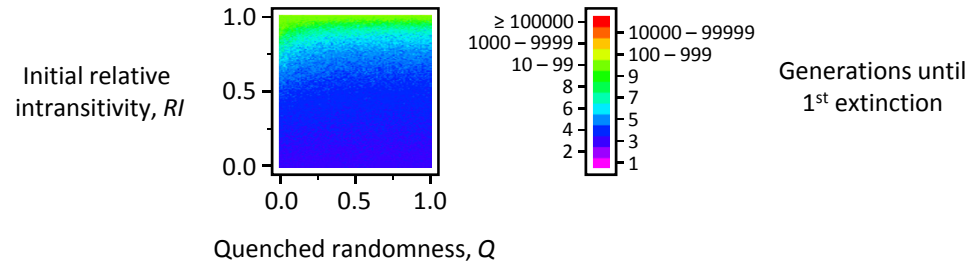


Fig. A4. [Subsequent page]. Each panel gives, for particular combinations of the number of neighbours per individual (k ; *columns*) and initial strategy richness (s ; *rows*), the proportion of simulation runs that became monocultures within 10^5 generations (across all tested values of initial RI) for values of Q between 0 and 1 in increments of 0.01. Q_c was estimated as the lowest value of Q for (and above) which more than 70% of the initial RI values examined resulted in monoculture (70% lines shown for visual reference).

Fig. A4

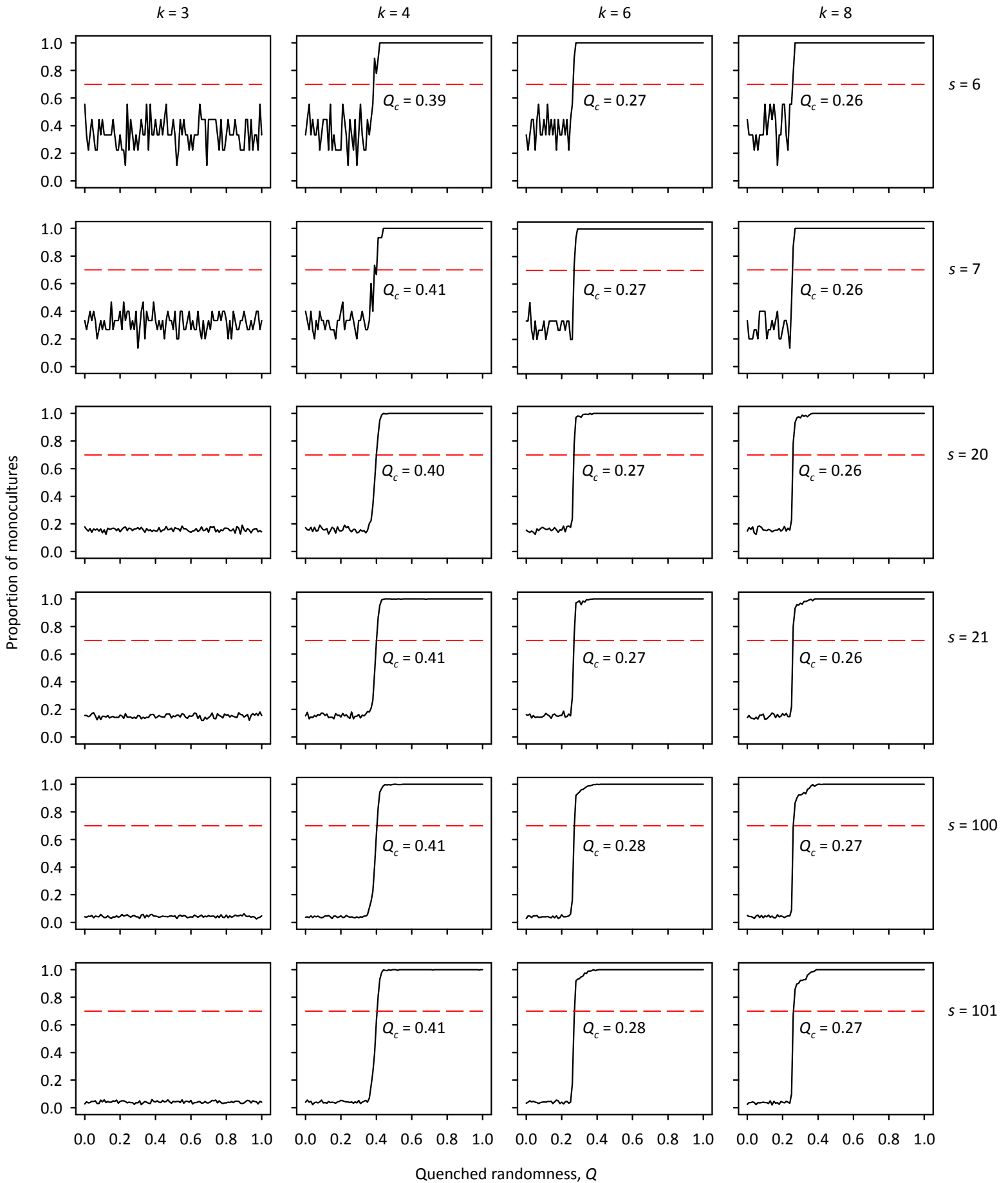


Fig. A5. [Subsequent page]. Generations until first extinction (*top row*), final strategy richness (r ; *second row*), final strategy evenness (E_{var} , *third row*), and final relative intransitivity (RI , *bottom row*) as a function of the number of neighbours per individual (k ; *columns*), initial relative intransitivity (RI), and quenched randomness (Q). Population size: $N = 10000$; initial number of strategies: $s = 101$. Each pixel represents a single model run. Interpretation of colours is given in the legends. (In the *bottom row*, white regions correspond to situations where $r < 3$, meaning that RI is undefined.)

Fig. A5

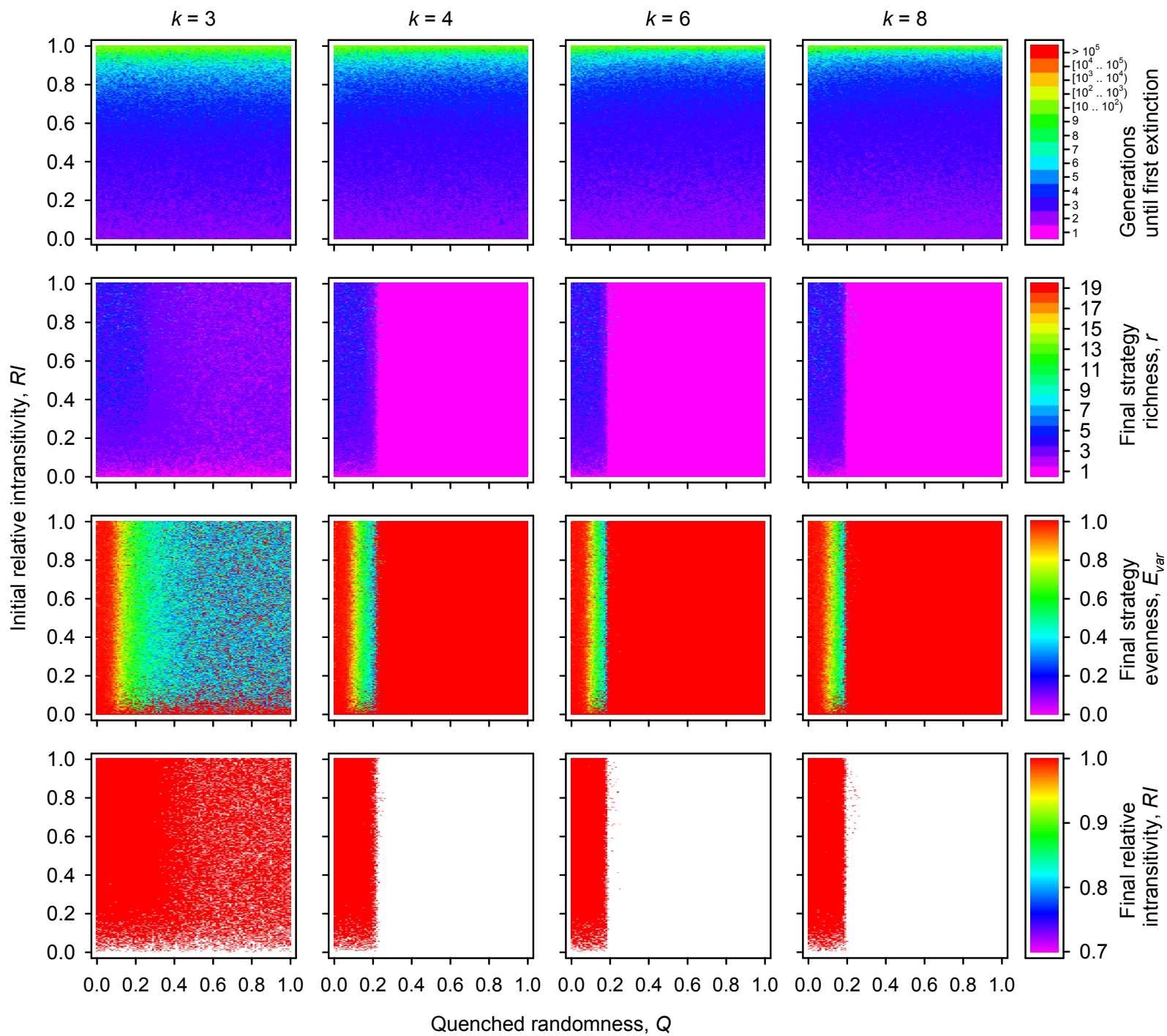


Fig. A6. [Subsequent page]. Relative area (A ; red) and strategy evenness (E_{var} ; blue) as a function of quenched randomness (Q ; *horizontal axis*), number of neighbours per individual (k ; *columns*), and population size (N ; *rows*). In every case, $s = 3$ and $RI = 1$ (i.e., intransitive three-strategy assemblages). A is estimated as the proportion of the area of the equilateral-triangular phase space that is filled with a convex hull surrounding the population trajectory between model generations 90001 and 100000 (e.g., the outermost outlines of the trajectories in the phase diagrams in Fig. 3). E_{var} is estimated as the average E_{var} over the same range of model generations. Symbols give the results of individual runs; there are 10 replicates for each value of Q between 0 and 1, inclusive, in increments of 0.01. Lines join the average values for each unique value of Q examined.

For $k = 4, 6,$ and 8 , A increases with Q , indicating that the amplitude of population oscillations becomes progressively greater. At Q_c , A abruptly decreases to 0; in the region beyond Q_c , the amplitude of population oscillations is so great that two of the three strategies go extinct before generation 90001, and the population trajectory subsequently remains static at one of the three corners of the phase space ($A = 0$). Concomitantly, E_{var} decreases with Q , indicating increasing disparity in the relative abundance of the three strategies. At Q_c , E_{var} abruptly increases to 1; monocultures have an evenness of 1 by definition. Note that in the smaller populations ($N = 10000$; *top row*) the increase in A and the decrease in E_{var} with Q are both rapider than in the larger populations ($N = 62500$, the same size as those highlighted in the main text; *bottom row*). Thus, the onset of violent population fluctuations sufficient to cause extinction depends on population size; i.e., Q_c is positively related to N , at least within the region of N values examined here.

For $k = 3$, the situation is slightly different, in that $N = 62500$ is a sufficiently large population to ensure that fluctuations never become sufficiently large to result in strategy extinctions within 100000 generations. This explains why there was no observed Q_c value for $k = 3$ interaction graphs in the main results. With smaller populations ($N = 10000$), the increase in amplitude of population oscillations is great enough to allow for occasional strategy extinctions starting at $Q = 0.38$. However, even beyond this value of Q , most model runs result in three-strategy coexistence. Presumably, a consistently measurable Q_c for $k = 3$ interaction graphs only comes into play at even smaller population sizes.

Fig. A6

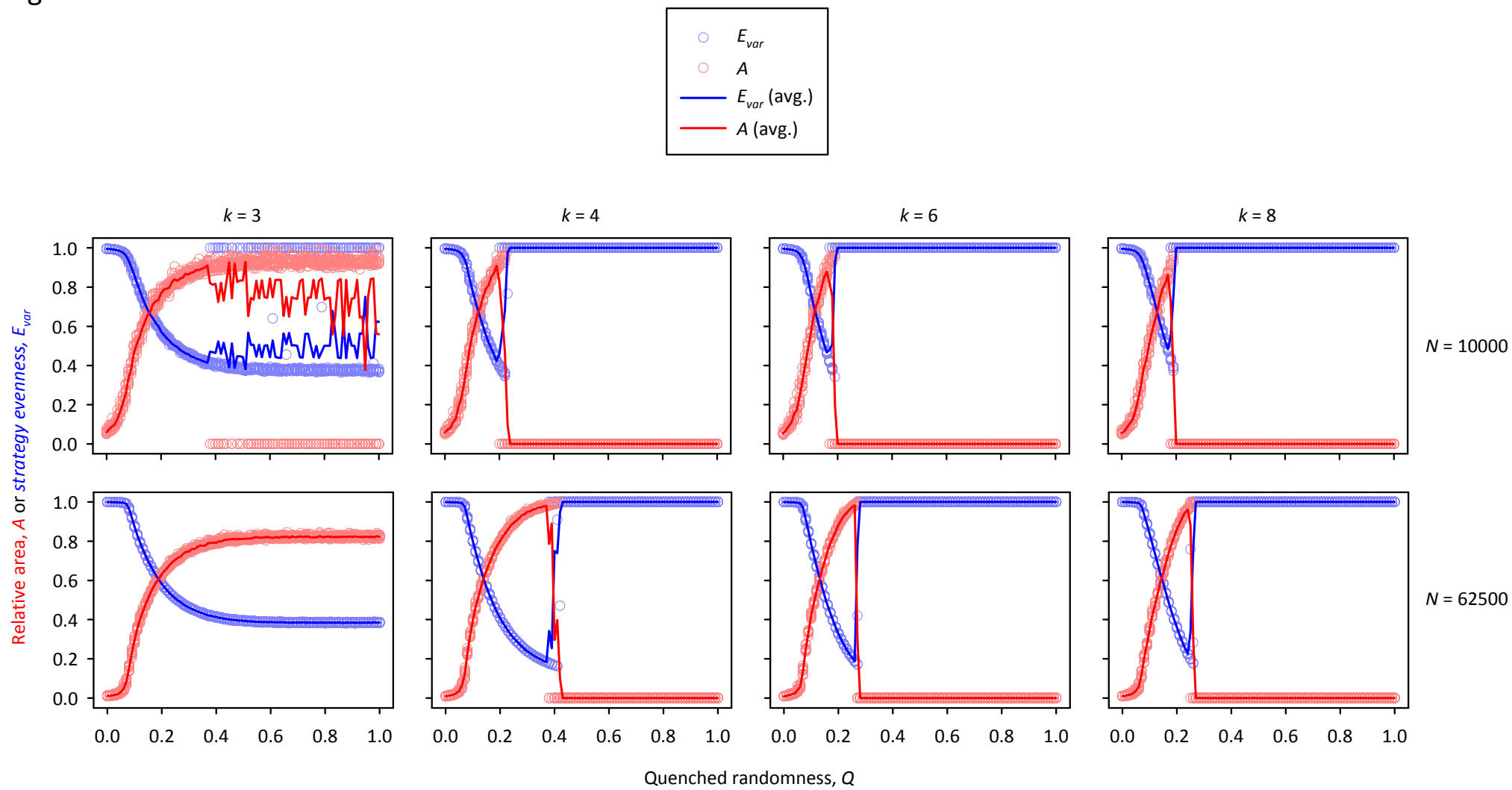


Fig. A7. [Subsequent page]. *Top row:* Relative area (A) as a function of population size (square root-transformed, $L = N^{0.5}$; *horizontal axis*) and number of neighbours per individual (k ; *panels*). In every case, $s = 3$, $RI = 1$, and $Q = 1$ (i.e., intransitive three-strategy assemblages interacting on regular random graphs). A is estimated as the proportion of the area of the equilateral-triangular phase space that is filled with a convex hull surrounding the population trajectory between model generations 90001 and 100000 (e.g., the outermost outlines of the trajectories in the phase diagrams in Fig. 3). Symbols give the results of individual runs; there are 10 replicates for each of $L = 10, 50, 100, 150, 200, 250, 300, 350, 400, 450, 500, 550, 600, 650, 700, 750, 800, 850, 900, 950,$ and 1000 (i.e., population sizes spanning $N = 100$ to 10^6). There are a further 10 replicates each for $L = 50$ to 150 for $k = 3$ and between $L = 400$ to 600 for $k = 4$, in increments of 2, to characterize the transitions from monoculture to coexistence with greater resolution. Lines join the average values for each unique value of N examined.

When N is relatively small, the large fluctuations that accompany rock-paper-scissors competition on regular random graphs (i.e., $Q = 1$) result in the extinction of two of the three strategies ($A = 0$). However, when N is sufficiently large, even these large fluctuations do not preclude strategy coexistence. Just what constitutes ‘sufficiently large’ is highly dependent on k , the number of neighbours per individual. When $k = 3$ rock-paper-scissors coexistence is predicted to be more likely than monoculture when the population size is greater than approximately $N = 8876$ (i.e., according to logistic regression; *bottom row*). For $k = 4$, the switch occurs at approximately $N = 206297$ (*bottom row*). Evidently, for $k = 6$ and 8 , the population sizes needed to allow coexistence in this scenario are rather greater: $N > 10^6$. Together, these findings help explain why in the main results, in which $N = 62500$, critical values of Q were evident for $k = 4, 6,$ and 8 , but not $k = 3$ (Fig. 1, Table 1). More broadly, it is evident that the existence of a critical quenched randomness is a phenomenon of finite population sizes. This makes Q_c particularly relevant to biological systems which are themselves finite and often small (compared to physical systems with extremely large N).

Fig. A7

